Separation and Purification Technology 251 (2020) 117280

Contents lists available at ScienceDirect

Separation and Purification Technology

journal homepage: www.elsevier.com/locate/seppur

Effect of (TiO_2: ZnO) ratio on the anti-fouling properties of bio-inspired nanofiltration membranes

Raúl Bahamonde Soria[a,e,*], Junyong Zhu[b,d], Irma Gonza[c], Bart Van der Bruggen[d], Patricia Luis[e]

[a] Renewable Energy Laboratory, Faculty of Chemical Sciences, Central University of Ecuador, Quito, Ecuador
[b] School of Chemical Engineering and Energy, Zhengzhou University, Zhengzhou 450001, PR China
[c] Department of Food Sciences, Laboratory of Food Analysis, Faculty of Veterinary Medicine, University of Liège, bât. B43bis, 10 Avenue de Cureghem, Sart-Tilman, 4000 Liège, Belgium
[d] Department of Chemical Engineering, KU Leuven, Celestijnenlaan 200F, B-3001 Leuven, Belgium
[e] Materials & Process Engineering (iMMC-IMAP), UCLouvain, Place Sainte Barbe 2, 1348 Louvain-la-Neuve, Belgium

ARTICLE INFO

Keywords:
Anti-fouling
Uv-photocatalysis
TiO_2 nanoparticles
ZnO nanoparticles
Dopamine
Nanofiltration membrane

ABSTRACT

Membrane fouling and biofouling, which arises from the nonspecific interaction between the membrane surface and foulants, significantly impedes the efficient application of membrane technology. The addition of nanoparticles could have an impact on the properties of membranes used for nanofiltration. Nanoparticles can provide various functionalities to a membrane but, there are very few studies of the effect of mixing catalysts in PDA-modified membranes. In this study, polydopamine has been used to firmly bind a combination of nanoparticles on thin film composite (TFC) membranes. Two simple methods (a one-step and a two-step method) to assemble a multifunctional (TiO_2, ZnO) layer of nanoparticles onto a commercial NF membrane as support have been evaluated by applying fast deposition of polydopamine (PDA). The membrane performance was evaluated based on the relative flux decline.

Results show that the modification methods did not compromise the rejection of $MgSO_4$, combined with an increase ~15% in the rejection of NaCl. A 25% increase in the hydrophilicity of the modified membranes compared to pristine membrane was evidenced. In addition, the two-step modification method has antimicrobial activity for an ultralow load of 0.03 wt% ZnO nanoparticles; the antimicrobial activity increased when the membrane had a combination of TiO_2:ZnO nanoparticles at 1:2 and 2:1 ratios using *Bacillus Subtilis* as model bacteria. The photocatalytic activity of the nanoparticles layer was demonstrated through the removal of methylene blue from a solution contacting the membrane when exposed to solar radiation.

1. Introduction

Nanofiltration (NF) is widely used for water treatment and wastewater reclamation/reuse [1,2]. NF membranes have properties in between those of ultrafiltration (UF) and reverse osmosis (RO). They are used in a wide range of different applications, such as rejecting ions, removal of heavy metals and of organic pollutants [2,3].

Several studies have shown that properties such as the desalting degree, porosity, membrane morphology, charge, membrane hydrophobicity, MWCO, molecular size, charge, hydrophobicity of the solute as well as the feed water chemistry have a direct influence on the permeability, rejection, colloidal fouling and biofouling behavior of RO and NF membranes [1,4–8].

Membrane fouling increases operation and maintenance costs by deteriorating the membrane performance and ultimately shortening the membrane lifetime [4]. Thus, it is of utmost importance to manufacture membranes that are resistant to fouling. One of the most extended methods to produce NF membranes is via interfacial polymerization. However, conventional manufacture methods involve tedious and complicated steps. In addition, the method for manufacturing membranes may considerably affect the anti-fouling capacity of the membranes.

Recently, there has been an increasing interest in bioinspired modifications, such as the mussel-inspired chemistry of polydopamine (PDA) for membrane surface modification [9,10]. Polydopamine coatings have been extensively used to change the surface properties of membranes for use in desalination[11–13], microbial fuel cells [14], wastewater treatment,[13] oil/seawater separation, [15] electrodialysis, [16] membrane bioreactors,[17] inter alia. These coatings have been shown to increase hydrophilicity and under water

* Corresponding author at: Renewable Energy Laboratory, Faculty of Chemical Sciences, Central University of Ecuador, Quito, Ecuador.
E-mail address: rabahamonde@uce.edu.ec (R. Bahamonde Soria).

https://doi.org/10.1016/j.seppur.2020.117280
Received 16 November 2019; Received in revised form 15 March 2020; Accepted 5 June 2020
Available online 21 June 2020
1383-5866/

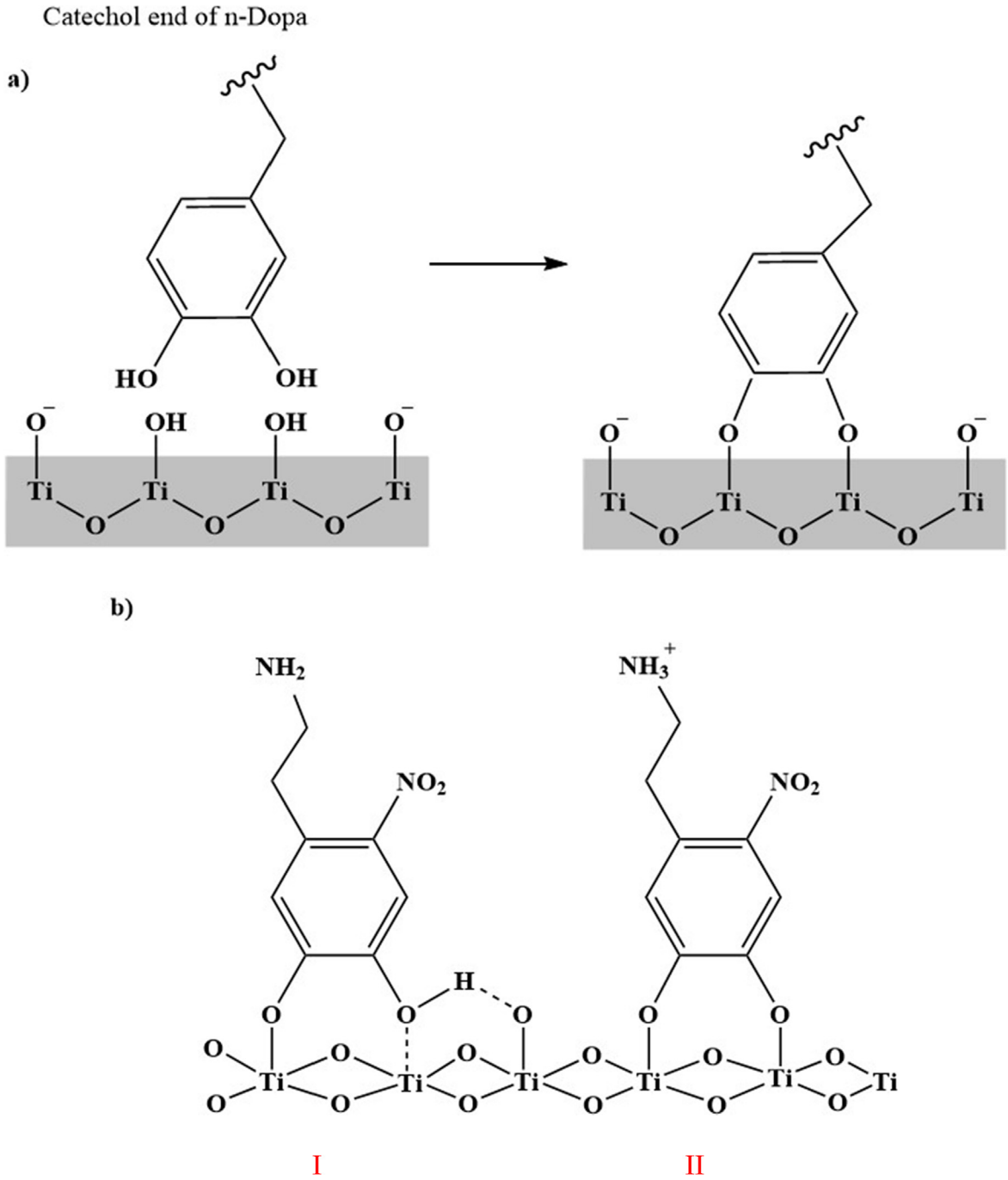

Scheme 1. Possible configurations of PDA adsorbed on TiO_2: (a) possible mechanism of mPEG-DOPA binding to TiO_2 surfaces; (b) possible configurations: (I) monodentate binding with a hydrogen bridge to a neighboring surface hydroxide and (II) bidentate binding.

oleophobicity of many hydrophobic membrane surfaces, which can result in improved membrane performance [13–15,17,18] and decreased microbial adhesion [14,17,19–21].

PDA has been used due to its high material-independent adhesion and post-functionalization accessibility [22], in order to greatly accelerate the polymerization of dopamine and the deposition rate of PDA has been used $CuSO_4$ /H_2O_2 as a trigger [23]. $CuSO_4$ /H_2O_2 can generate reactive oxygen species (ROS) in an alkaline medium to improve the deposition rate of PDA coatings with high uniformity and stability, which greatly expands the potential of PDA in practical applications [24]. Adding organic nanoparticles such as graphite oxide or inorganic nanoparticles such as TiO_2, SiO_2, Al_2O_3, Si, Ag, ZnO, ZrO_2, etc. into the thin film have had significant effects on the membrane performance [25] and on fouling resistance [26,27].

Dopamine can react with metal oxide nanoparticles surface through surface complexation by any of these routes: (1) via catechol as a bidentate bonding [28]; (2) bridged bidentate bonding [29]; and (3) complex mechanism as monodentate-bidentate bonding or hydrogen bonding [30,31] (Scheme 1). These photocatalysts deposited on the surface could help to degrade contaminants such as drugs or dyes [32] if the modified membranes are irradiated with UV light. The presence of nanoparticles could also have an influence on the fouling resistance of the membranes [33].

Furthermore, the anchoring of catalyst nanoparticles on membrane surfaces allows these nanomaterials to maintain maximum contact with natural organic matter, proteins and bacteria, which could reduce their

Table 1
Comparison of the catalyst concentration on the modified surface membrane.

Support/Membrane	Film – Nanoparticles	Solution catalyst concentration (%)	Propriety of membrane	Modification method	Ref.
PES	MPD/FeO	0.05–0.2	Water treatment Anti-fouling activity	Pre-seeding interfacial polymerization method	[37]
RO-PSF	PDA/AgNanoparticles	1	Anti-microbial modification	PDA coating and in situ formation of AgNanoparticles	[38]
FO-PA TFC	PDA- Mg_3 Al-CO_3(LDH)	0.1	Chlorine and fouling resistance	Two modification strategies as deposition and dip-coating were compared.	[39]
PU nanofibers	PDA-ZnO	0.5	Photocatalytic and antimicrobial	Combining of electrospinning, surface functionalization and hydrothermal treatment	[40]
Carboxymethyl cellulose	Chitosan-ZnO	0.5–2	Antifungal properties	Casting method	[41]
PAN UF sheet membranes	PDA – Cu	0.3	Elevated salt transport of antimicrobial membrane	Two-step deposition and co-deposition	[24]
UF PI	Co-polyamide TiO_2	0.05	Solvent resistant nanofil-tration membranes	In situ interfacial incorporation of TiO2 nanoparticles along with fabrication of co-polyamide network on a polyimide (PI) support.	[42]
PES	PDA - TiO_2	0.1–0.5	Good hydrophilic performance	Two-step deposition	[35]
PVD	PVDF - (TiO_2@PDA) Nanoparticles	1	Multiple antifouling capacities	Hybrid membranes fabricated by non-solvent induced phase in-version (NIPS)	[43]
NF PA -TFC	PDA - TiO_2 PDA - ZnO PDA–TiO_2:ZnO	0.01–0.05	Photocatalytic antifouling activity	Two-step deposition and co-deposition)	This Work

adhesion and growth. The different nanoparticles on the surface of the membrane could be intimately related to an improvement in membrane performance. For this reason, some research has focused on modification of NF membranes with different nanoparticles (Table1) [34–36].

In this study, we have introduced and compared two simple methods to assemble a multifunctional (TiO_2, ZnO) layer of nanoparticles onto a commercial NF membrane as support by applying the fast deposition of PDA. One of these techniques refers to a conventional two-step deposition by the aid of a strongly adhesive PDA intermediate layer followed by nanoparticles loading. The second strategy is the simultaneous co-deposition of PDA and nanoparticles. The influence of the catalyst (TiO_2, ZnO and mixtures) and the two modification strategies are compared and studied taking into account surface morphology, selectivity for specific solutes and permeability. The antimicrobial activity of the membranes is also studied by using *Bacillus Subtilis* as model bacteria.

2. Experimental

2.1. Materials

A commercial polyamide nanofiltrationmembrane, NFX (150–300 Da), was purchased from Synder filtration (USA). Dopamine hydrochloride (99 wt%) and tris(hydroxymethyl) aminomethane (Tris, 99.8% by weight) were acquired from Acros Organic-Belgium. Copper (II) sulfate ($CuSO_4$, 99 wt%), hydrogen peroxide (H_2O_2, 30 wt%), hydrochloric acid (HCl, 1 M) and sodium hydroxide (NaOH, 98 wt%), titanium (IV) oxide nanopowder (anatase, < 25 nm, 99.7 wt%), zinc oxide (ZnO, < 50 nm 99 wt%), magnesium sulfate ($MgSO_4$, 98 wt%) and sodium chloride (NaCl, 99 wt%), were acquired from Sigma-Aldrich (Diegem, Belgium). Unless specified, all solutions were prepared in deionized (DI) water purified by a Milli-Q ultrapure unit. All reagents and solvents were commercially available and used as received.

The culture media Iso Sensitest Broth (Oxoid CM 0473) containing 0.8 wt% Agar bacteriological N° 1 (Oxoid LP0011) was used for growing *Bacillus Subtilis* (BGA) spore suspension (Merck 1.10649). The media was sterilized at 121 °C for 45 min and cooled down to 45–50 °C before adding 0.4 wt% of glucose and B. Subtilis strain at the required concentration.

2.2. Modification of the NFX nanofiltration membrane

NFX-TFC membranes (NF) were used for all surface modification procedures. The commercial NF membranes were immersed in distilled water for 12 h before surface modification. In addition, all the membranes used in this study were stored in distilled water until use.

The methodology used to modify the membranes has been reported by Zhang et al. [34]. Two methods have been studied: (1) fast co-deposition of PDA, in which catalyst nanoparticles are added in one step with the PDA according to compositions in Table 2, and (2) binding method in two steps, in which a fast PDA deposition on the NF membrane surface is followed by binding catalyst nanoparticles at different compositions (Table 2) on PDA modified NF membranes. The surface modification of NF membranes was done in a membrane holder.

2.2.1. One step - fast co-deposition procedure

Copper sulfate (8.3 mM) was dissolved in 30 mL Tris buffer solution (50 mM, pH 8.5); then, the catalyst amounts indicated in Table 2 for the membranes NF-Xa were added in this suspension. The resulting suspension was agitated during 3 h at 1000 rpm and subsequently, the suspension was further treated using sonication for 1 h in a water bath (20 °C). Next, 40 μL H_2O_2 solution (19.6 mM) was added into the suspension as the trigger of the rapid deposition and mixed, which was followed by the addition of dopamine hydrochloride (2 mg * mL^{-1}).

The solution was then poured onto the membrane surface in the

Table 2
Preparation conditions of modified membranes: (i) co-deposition method (one step modification), indicated as NF-Xa membranes, and (ii) binding method (two steps modification), indicated as NF-Xb membranes.

	Membrane	Dopamine (mg*mL^{-1})	TiO_2 Content (wt%)	ZnO Content (wt%)	Deposition PDA time (h)	Catalyst co-deposition time (h)	(TiO_2:ZnO) Ratios
	NF						
	NF-PDA	2	0	0	1	0	–
NF-1	NF-1a	2	0.01	0	1	0	–
	NF-1b	2	0.01	0	1	1	–
NF-2	NF-2a	2	0.03	0	1	0	–
	NF-2b	2	0.03	0	1	1	–
NF-3	NF-3a	2	0.05	0	1	0	–
	NF-3b	2	0.05	0	1	1	–
NF-4	NF-4a	2	0	0.01	1	0	–
	NF-4b	2	0	0.01	1	1	–
NF-5	NF-5a	2	0	0.03	1	0	–
	NF-5b	2	0	0.03	1	1	–
NF-6	NF-6a	2	0	0.05	1	0	–
	NF-6b	2	0	0.05	1	1	–
NFX-1	NF-X1a	2	0.005	0.005	1	0	1:1
	NF-X1b	2	0.015	0.015	1	1	1:1
NFX-2	NF-X2a	2	0.003	0.007	1	0	1:2
	NF-X2b	2	0.010	0.020	1	1	1:2
NFX-3	NF-X3a	2	0.007	0.003	1	0	2:1
	NF-X3b	2	0.020	0.010	1	1	2:1

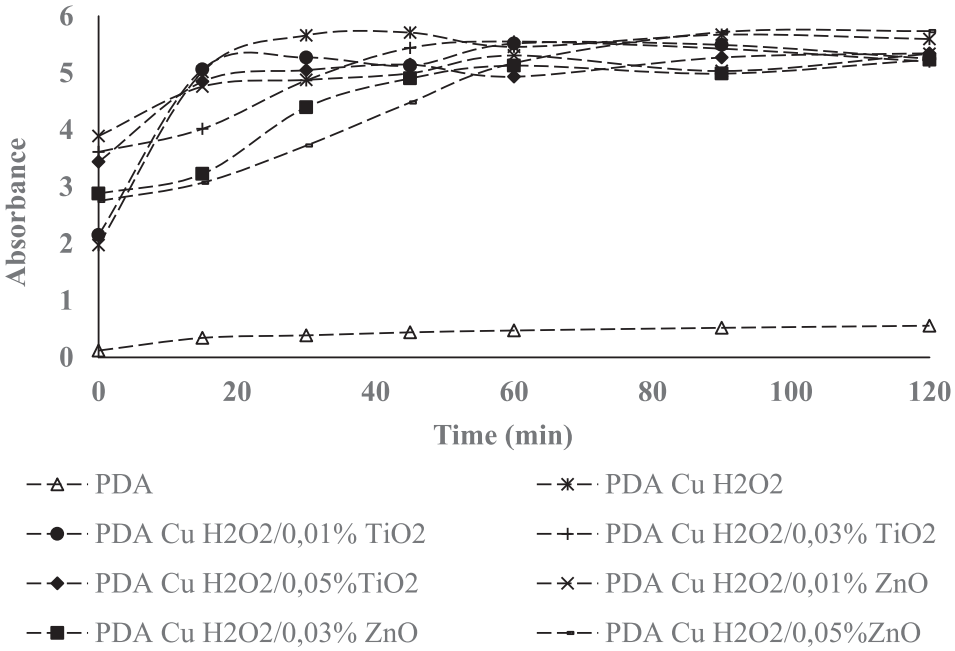

Fig. 1. Polymerization time analysis: UV–Vis absorbance at 403 nm for dopamine solutions (a) PDA solutions without $CuSO_4/H_2O_2$ (b) PDA + $CuSO_4/H_2O_2$, (c) PDA + $CuSO_4/H_2O_2$/ 0.01%TiO_2, (d) PDA + $CuSO_4/H_2O_2$/ 0.03%TiO_2, (e) PDA + $CuSO_4/H_2O_2$/ 0.05%TiO_2, (f) PDA + $CuSO_4/H_2O_2$/0.01%ZnO, (g) PDA + $CuSO_4/H_2O_2$ /0.03%ZnO, (h) PDA + $CuSO_4/H_2O_2$/0.05%ZnO. The dashed lines are added to guide the eye.

membrane holder for 1 h. Afterwards, the membrane was rinsed 5 times with distilled water to remove the excess polymerization residues and catalysts.

2.2.2. Two steps modification- binding procedure

An aqueous solution of dopamine was prepared by dissolving dopamine hydrochloride (2 mg*mL^{-1}) in Tris buffer solution (pH 8.5, 50 mM). In 30 mL of this fresh dopamine aqueous solution, $CuSO_4$ (8.3 mM) was dissolved with 40 μL H_2O_2 (19.6 mM). The final solution was poured onto the membrane surface placed in the membrane holder. After 60 min, the membrane was rinsed using distilled water for 5 min in order to remove most of the residual unbound polydopamine. Afterwards, the membranes were dried by compressed air for 5 min [34,44].

As the second step, different amounts of TiO_2 and ZnO nanoparticles (Table 2 - membranes NF-Xb) were added to a Tris buffer solution (pH 8.5, 10 mM) and agitated for 3 h at 1000 rpm by using a magnetic stirring plate. The suspensions of TiO_2 and ZnO nanoparticles and the mixtures were further treated by sonication for 1 h in a water bath (20 °C) to obtain a well dispersed suspension of nanoparticles. The prepared catalysts suspensions (30 mL) were added over the PDA modified NF membrane in the membrane holder and placed for 1 h at room temperature to allow the deposition of nanoparticles on the membrane surface. Afterwards, the membranes were carefully removed from the membrane holder and rinsed five times with distilled water.

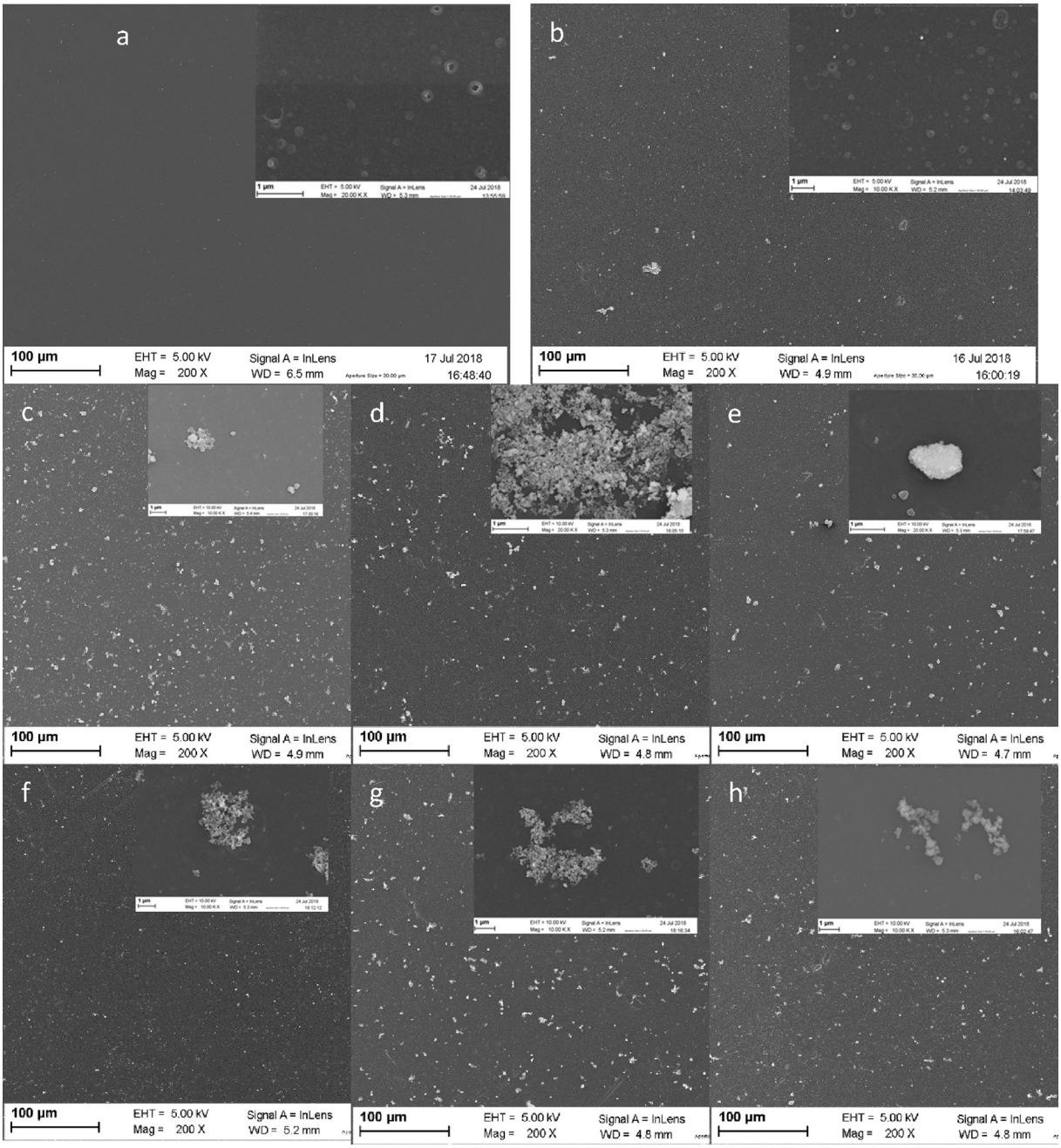

Fig. 2. Surface SEM images of membranes using the co-deposition method (one-step): (a) Pristine, (b) NF-PDA, (c) NF-1a, (d) NF-2a, (e) NF-3a, (f) NF-4a, (g) NF-5a, (h) NF-6a.

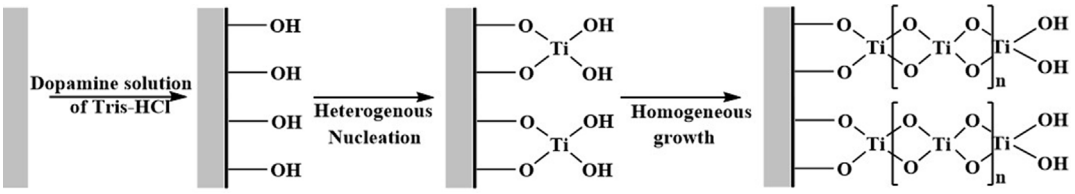

Scheme 2. A scheme of TiO_2 deposition on the polymer substrates mediated by PDA [22,55].

2.3. Membrane characterization

2.3.1. Surface morphology

The morphology of the membrane surface was evaluated by scanning electron microscopy (SEM) (Philips XL30-FEG) composed of an energy dispersive X-ray (EDX) detector. Each sample was dried before analysis in a vacuum chamber. Then, the membranes were submerged in liquid N_2 and fractionated, and afterwards they were coated with graphite.

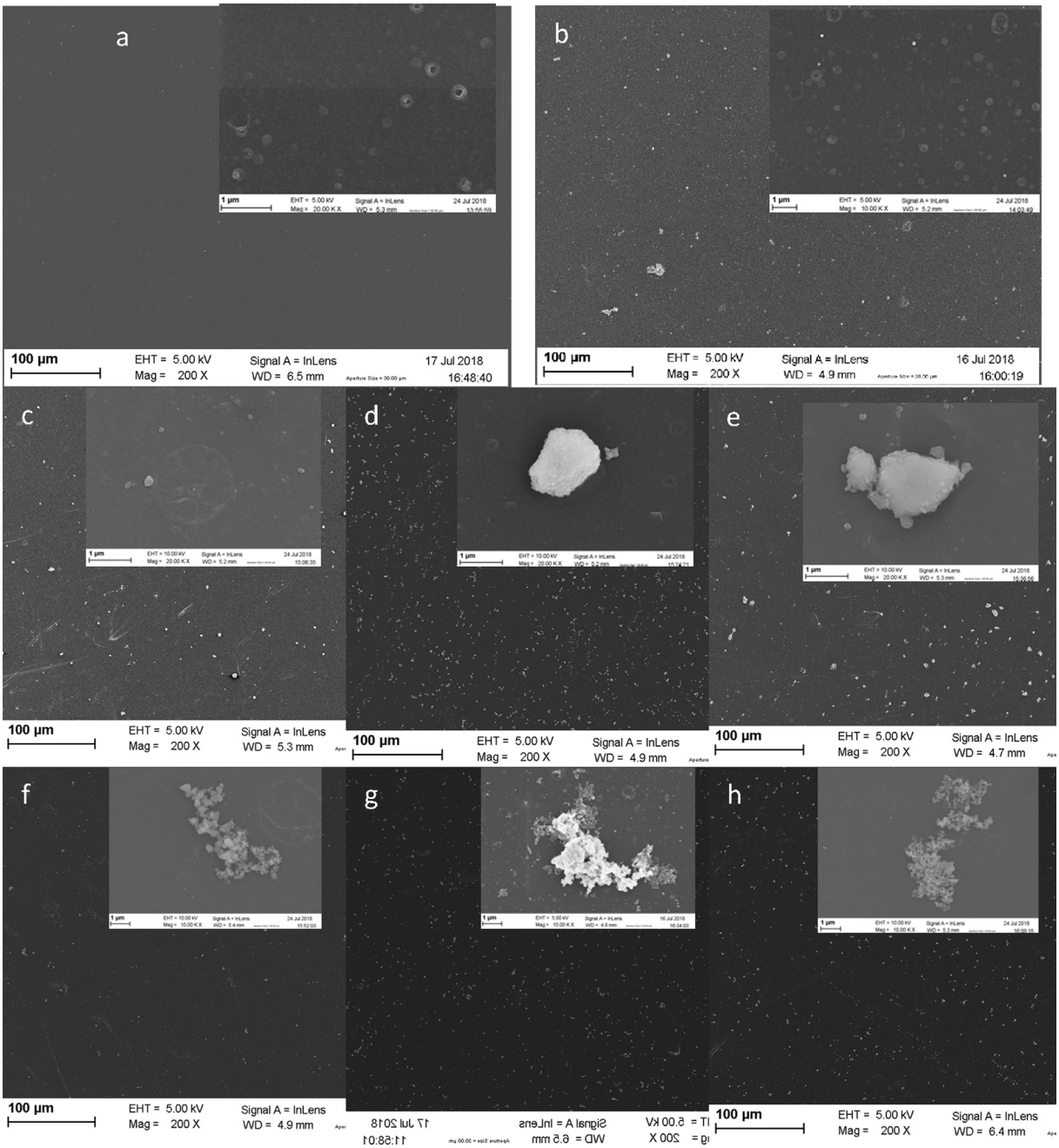

Fig. 3. Surface SEM images of the membranes with the binding method (two steps) (a) Pristine, (b) NF-PDA, (c) NF-1b, (d) NF-2b, (e) NF-3b, (f) NF-4b, (g) NF-5b, (h) NF-6b.

2.3.2. Water contact angle

Water contact angle measurements were measured to evaluate the hydrophilicity of the modified membranes. A contact angle goniometer (OCA20, Dataphysics Instruments, Germany) was used. A drop of distilled water (2.0 µL) was placed on the membrane surface. Static contact angles were measured using a circle fitting method by the drop shape analysis software.

2.3.3. Filtration performance test

Water flux and salt retention were characterized using a steel dead-end cell (HP4750 High Pressure Stirred Cell Kit). Membrane samples were tested at 4 bar. The water flux (J), water permeability (P_w) and rejection (R) of prepared membranes were calculated using the following equations:

$$J = V/(A\Delta t) \tag{1}$$

$$P_w = J/\Delta p \tag{2}$$

$$R = (1 - C_p/C_f) \times 100\% \tag{3}$$

where V is the volume of permeate (L), A is the effective membrane area (22.9 cm^2), Δt is the filtration time (h) and Δp is the applied pressure (bar). C_p and C_f are the salt concentrations of permeate and feed solutions (g L^{-1}) and were measured with an electrical conductivity meter (Thermo Scientific Orion Star A212). The dead-end cell was filled with 200 mL of solution (1 g L^{-1} NaCl and 1 g L^{-1} $MgSO_4$ in distillate water) and tested at room temperature. Once the membrane system reached a steady state, the permeate was collected. The solution into the dead cell was stirred at 800 rpm to reduce concentration polarization. The experiments were carried out in triplicate.

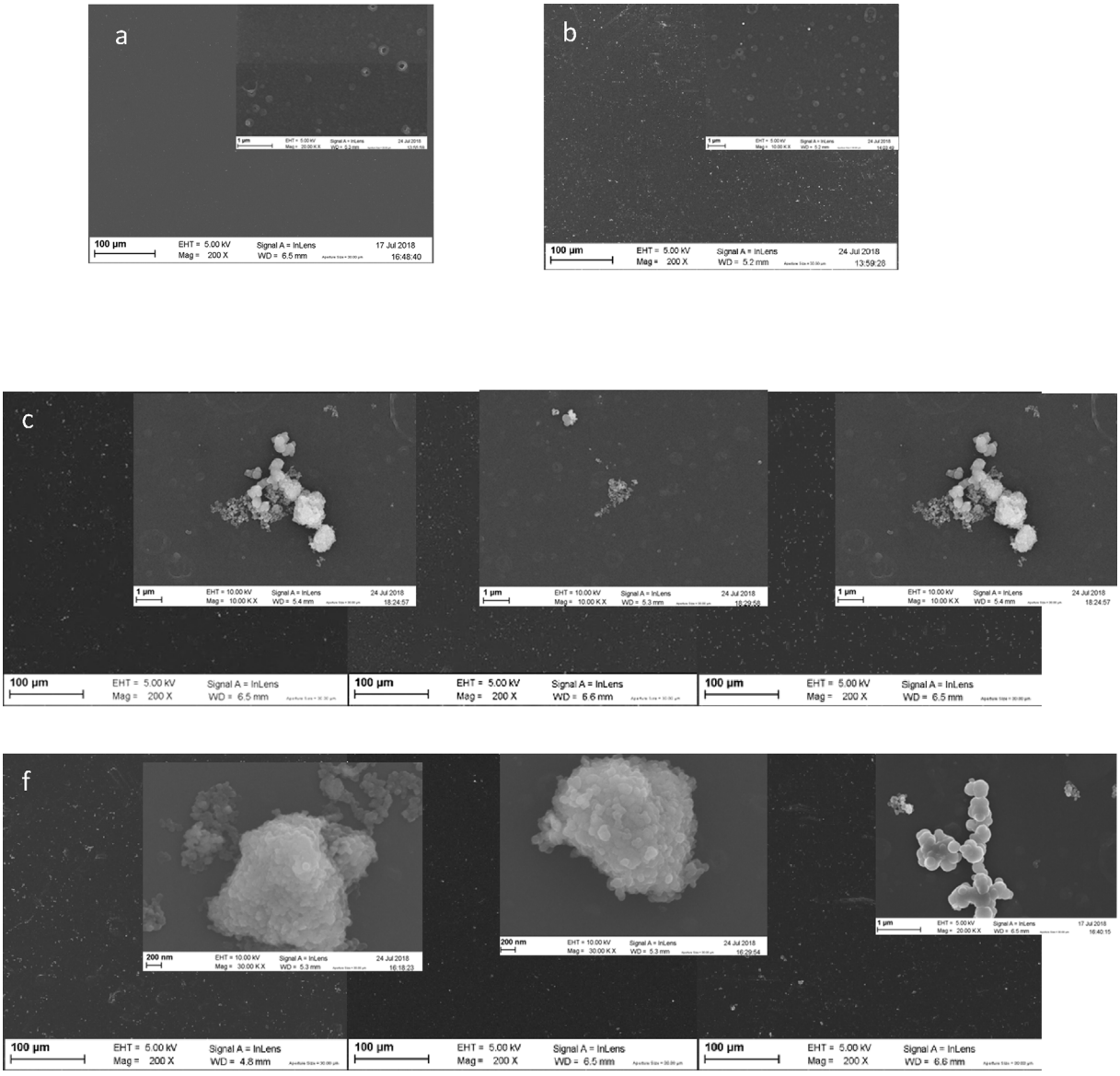

Fig. 4. Surface morphology of the (a) Pristine membrane; (b) NF PDA; PDA NFX Co-deposition method 0.01 wt% total mixture Nanoparticles, with ratios (TiO_2:ZnO): (c) 1:1 NFX-1a, (d) 1:2 NFX-2a (e), 2:1 NFX-3a. Two steeps - binding method 0.03 wt% total mixture nanoparticles, with ratios (TiO_2:ZnO) (f) 1:1 NFX-1b, (g) 1:2 NFX-2b, (h) 2:1 NFX-3b.

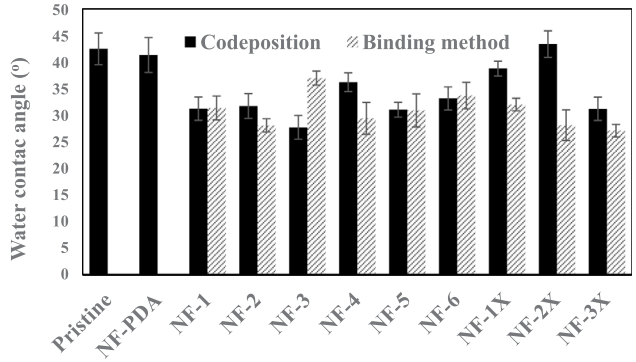

Fig. 5. Static water contact angles of the pristine and modified membranes.

2.4. Antibacterial capacity of modified membranes

2.4.1. Iso Sensitest

The modified method proposed by Khorshidi [45] was used to test the antibacterial activity of both the unmodified and modified membranes. An *Iso Sensitest* broth media containing *B. subtilis* spore suspension was incubated for 24 h at 32 °C in order to promote the bacterial growth. Either the unmodified and modified membranes were cut into pieces of 4.5 cm^2 and placed at the bottom of separate petri plates. Then, 2 mL of bacterial solution was carefully poured onto the membrane surface. Two UV lamps (254 nm, 6 W) were placed at a height of 10 cm from the open surface of petri plates. After 30 min of UV exposition over each membrane containing the 2 mL of bacterial solution. 30 µL of the solution covering the membrane surface were taken and diluted 10:1. The resulting solution was poured onto Petri plates of 90 mm containing 8 mL of *Iso Sensitest* broth media with 0.8% of Agar N°1 to solidification of the media. The plates were incubated for 18 h at 30 °C, the antibacterial property of the membrane was determined by the growing radius of each bacterial colony formed on the plates.

2.4.2. Disk diffusion method

A second type of antibacterial tests was performed via the disk diffusion method. The methodology proposed by Lashkenari [46] was

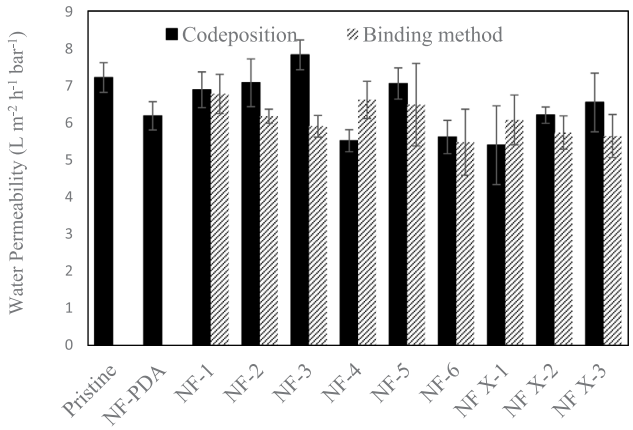

Fig. 6. Water permeability of the modified nanofiltration membranes using PDA and various TiO_2/ZnO ratios by binding and co-deposition methods; Pristine (NF), NF-PDA 0% wt catalyst, NF-1, 2 and 3, which have 0.01, 0.03 and 0.05%wt of TiO_2 respectively and NF-4, 5 and 6 which have 0.01, 0.03 and 0.05%wt of ZnO respectively and mixtures of catalyst, using two methods; co-deposition in total composition 0.01%wt (TiO_2:ZnO) ratios 1:1, 1:2 and 2:1 for NFX-1, 2 and 3 respectively, and binding method in total composition 0.03%wt (TiO_2:ZnO) ratios 1:1, 1:2 and 2:1 for NFX-1, 2 and 3 respectively.

followed. The culture media was seeded with *B. Subtilis* strain at a final concentration of 10^4 (colony forming units) CFU mL^{-1} and 0.4% of glucose before filling the sterile Petri dishes with 8 mL of prepared media. The prepared plates were stored at 4 °C and kept one week as maximum before use. For the evaluation of the antibacterial activity, disks of 1 cm^2 of modified and pristine membranes were placed on the plates and incubated for 18 h at 32 °C in dark conditions. Antibacterial capacity of each membrane was evaluated by the presence of an inhibition zone and size of the inhibition zone around the membranes.

2.5. Photocatalytic performance of membranes for dye degradation under light conditions

The photocatalytic activity of the prepared membranes was studied by degrading an aqueous solution of 10 mg L^{-1} methylene blue (99 wt %, Sigma Aldrich, supplied by Merck Ecuador). The degradation of methylene blue was tested under the influence of sunlight in Quito (Ecuador) between 10th September and 10th October 2018 [47]. The time period used in the evaluation was kept constant from 11:00 a.m. to 2:00 p.m. to standardize the UV irradiation [48]. The tests were performed when the UV Index in Quito - Ecuador started in 10, according to the Ecuadorian National Institute of Meteorology and Hydrology. The membranes (22.9 cm^2 membrane diameter) were exposed to light irradiation for 3 h in a membrane holder; 20 mL of dye aqueous solution were added in the membrane holder without magnetic stirring. After the adequate irradiation time, 5 mL of the solution was collected and analyzed using UV–Vis spectrophotometer at a wavelength of 662 nm. All experiments were made in triplicate reporting average values, with error below 5%.

The removal efficiency was evaluated using Eq. (4):

$$\%removalefficiency = \frac{C_0 - C}{C_0} x100 = \frac{A_0 - A}{A_0} x100 \quad (4)$$

where C_o and C are initial and final concentrations of methylene blue, respectively. A_o is the initial absorption and A is the final absorption of methylene blue.

3. Results and discussion

3.1. Polymerization time

Dopamine generally forms a thin hydrophilic and adherent coating by oxidation under alkaline conditions or spontaneously by self-polymerization [49]. However, the polymerization of dopamine is a slow process [50]. In this work, a rapid deposition strategy was used to speed up the process. All solutions underwent a rapid color change due to the influence of Cu^{2+} and H_2O_2 on the self-assembly of the thin polydopamine films. Cu^{2+} and H_2O_2 generate a multitude of reactive oxygen species in an alkaline medium (pH 8.5); these reactive oxygen species are added to the aromatic rings of the polydopamine and significantly accelerate the deposition rate of PDA coatings with high uniformity and stability [19].

Fig. 1 depicts the change of UV–Vis absorbance at 403 nm for various dopamine solutions. When $CuSO_4/H_2O_2$ was not added, the

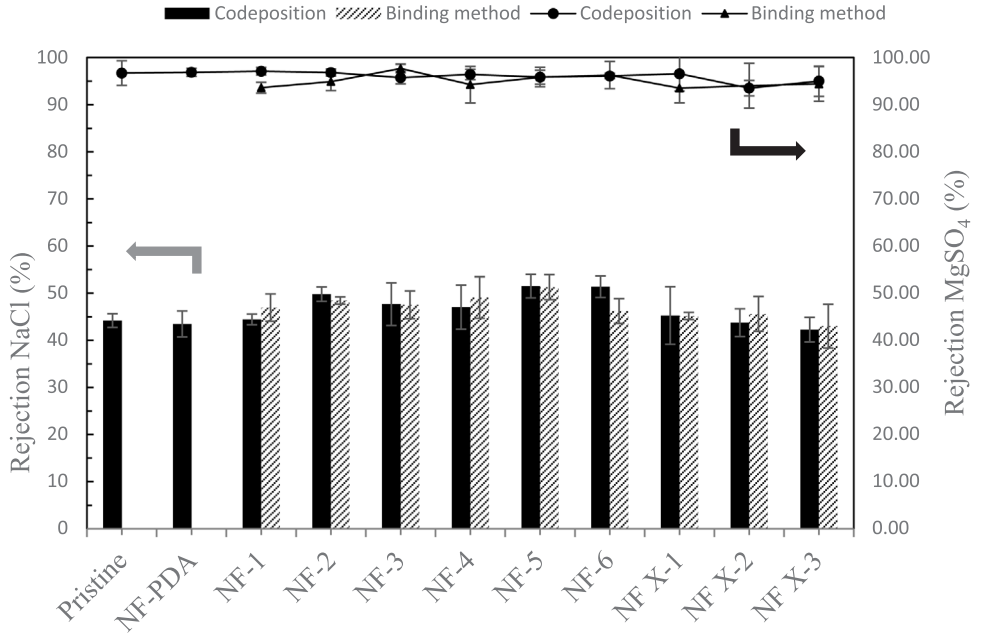

Fig. 7. % NaCl and $MgSO_4$ rejection of the unmodified and modified membranes with co-deposition method and two steps method in different concentration of catalyst and with various ratios of catalyst (TiO_2:ZnO), 1:1, 1:2 and 2:1 for NFX-1, 2 and 3 respectively.

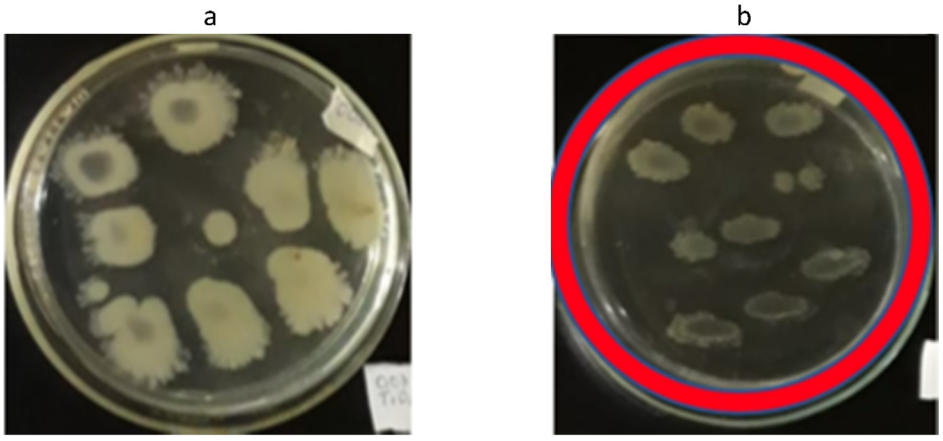

Fig. 8. Images of the *B. Subtilis* colonies formed in the plate of UV-treated (a) NF2b (0.03%w TiO_2), (b) NF-5b (0.03%wt ZnO), In modified by two steps membranes after 30 min of UV irradiation.

absorbance increases from 0.2 to 0.5, indicating that the polymerization has started. However, this polymerization method was less efficient than the solution with $CuSO_4/H_2O_2$. The absorbance was gradually increased from 2.80 to around 5.22 for all cases using $CuSO_4/H_2O_2$ in 60 min. This result confirms a fast polymerization using $CuSO_4$ as initiator. After this time, the value was remained constant, showing that the polymerization time of dopamine is completed in 60 min. A polymerization time of PDA in membranes around 60 min to achieve a complete polymerization was also observed in previous studies [34,36,51]. For this reason, the polymerization time was set at 60 min for all experiments. In addition, recent research have showed that this method could generate a homogeneous thickness close to 45 nm by moderate covalent polymerization of dopamine (C═C−C═O) [52], and it can form a stable PDA layer on the membrane surface [34,51]. Furthermore, Fig. S1 (A) presents the color change of various PDA solutions (see Table 2) over time. The color change is due to the oxidation of dopamine [49]. Solutions with $CuSO_4/H_2O_2$ turned to black within 20 min, and no visible particles were formed at this time, which indicates that in this time, the polymerization has started, and it is faster than that of the solution without $CuSO_4/H_2O_2$. The absorbance for solutions with $CuSO_4/H_2O_2$ and catalyst was gradually increased to 5.22 on average in 60 min. The absorbance of these solutions was much higher than solution of dopamine (0.44), because $CuSO_4$ oxidizes dopamine, and $CuSO_4/H_2O_2$ produces a large number of reactive oxygen species to trigger dopamine polymerization. Fig. S1(A) also showed visible deposits of polydopamine in the solutions after 30 min. This phenomeno was more evident in solutions with metallic oxides and it could be due to the sedimentation of nanoparticles covered with PDA, and hence, the sedimentation time of different catalysts was evaluated at a wavelength of 403 nm (Fig. S1B). From 50 min on, it is possible to see a stabilization in the absorbance of the solutions. For times over 60 min, sedimentation of particles is observed. For this reason, 60 min was considered the optimal time of polymerization.

3.2. Morphology of membrane surface

The polyamide layer was modified by embedding TiO_2 and ZnO nanoparticles. Dopamine can react with metal oxide nanoparticles surface through surface complexation by any of these routes (Scheme 1).

3.2.1. One-step method (co-deposition)

The SEM images in Fig. 2 confirm the change on the pristine NF surface with the one-step modification (co-deposition) method. The cross-section of the membranes can be observed in Fig. S2 in Supporting Information.

The nanoparticles are present on the surface of NF-PDA due to the reaction of the active functional groups (hydroxyl groups in catechol) of PDA with TiO_2 and ZnO nanocrystals [43,53–55] and homogeneous nucleation between metal oxides nanoparticles (Scheme 2) [55]. The excessive weight of the PDA coated nanoparticles is removed immediately after washing the membrane. However, the one-step method presented a limited amount of nanoparticles on the surface. The nanoparticles can be covered by PDA and form lumps on the surface of the membrane. In addition, two aspects could be also observed: (i) the TiO_2 nanoparticles adhere more efficiently in comparison with ZnO nanoparticles, and (ii) the size difference of nanoparticles is more evident as the concentration of catalyst increases from 0.03 to 0.05 wt% in comparison with 0.01 wt%, where the distribution and nucleation size of nanoparticles on the surface is more homogeneous (Fig. 2c and f). Concentrations of catalyst lower than 0.03% would thus give a homogeneous distribution on the surface during the copolymerization.

3.2.2. Two-step method (binding method)

The SEM images in Fig. 3 show the membrane surface after the two–step modification (binding) method. The surface of the modified membranes showed a wide range of nanoparticle sizes. This could be due to the heterogeneous nucleation followed by homogeneous nucleation of nanoparticles (Scheme 2). This phenomenon is more evident when the concentration of catalyst increases from 0.01% to 0.05% and with TiO_2. Previous research focused on concentrations of 0.05% TiO_2 [34,35,41]. However, our observations prove that a load of 0.03% has a more homogeneous distribution for the two studied metal oxides (TiO_2 and ZnO).

Fig. 3 and Fig. S2 show fewer ZnO nanoparticles on the membrane surface compared to TiO_2 nanoparticles. This can be explained by the fact that ZnO nanoparticles have only one oxygen atom in their structure and the heterogeneous nucleation with the PDA surface is not as efficient as with TiO_2 nanoparticles, which have two oxygen atoms [40].

3.2.3. One-step and two-step methods with TiO_2:ZnO mixtures

Fig. 4 represents images of the pristine membrane, modified membranes by co-deposition with 0.01 wt% total nanoparticles and ratios TiO_2:ZnO (1:1, 1:2, 2:1) and, modified membranes by binding with 0.03 wt% total nanoparticles and ratios TiO_2:ZnO (1:1, 1:2, 2:1). Membranes modified by the co-deposition method showed a better homogeneous nanoparticles distribution in the film in comparison with the binding method.

An EDX analysis was performed to also verify that the membranes were covered with catalysts Fig. S3 Supplementary data.

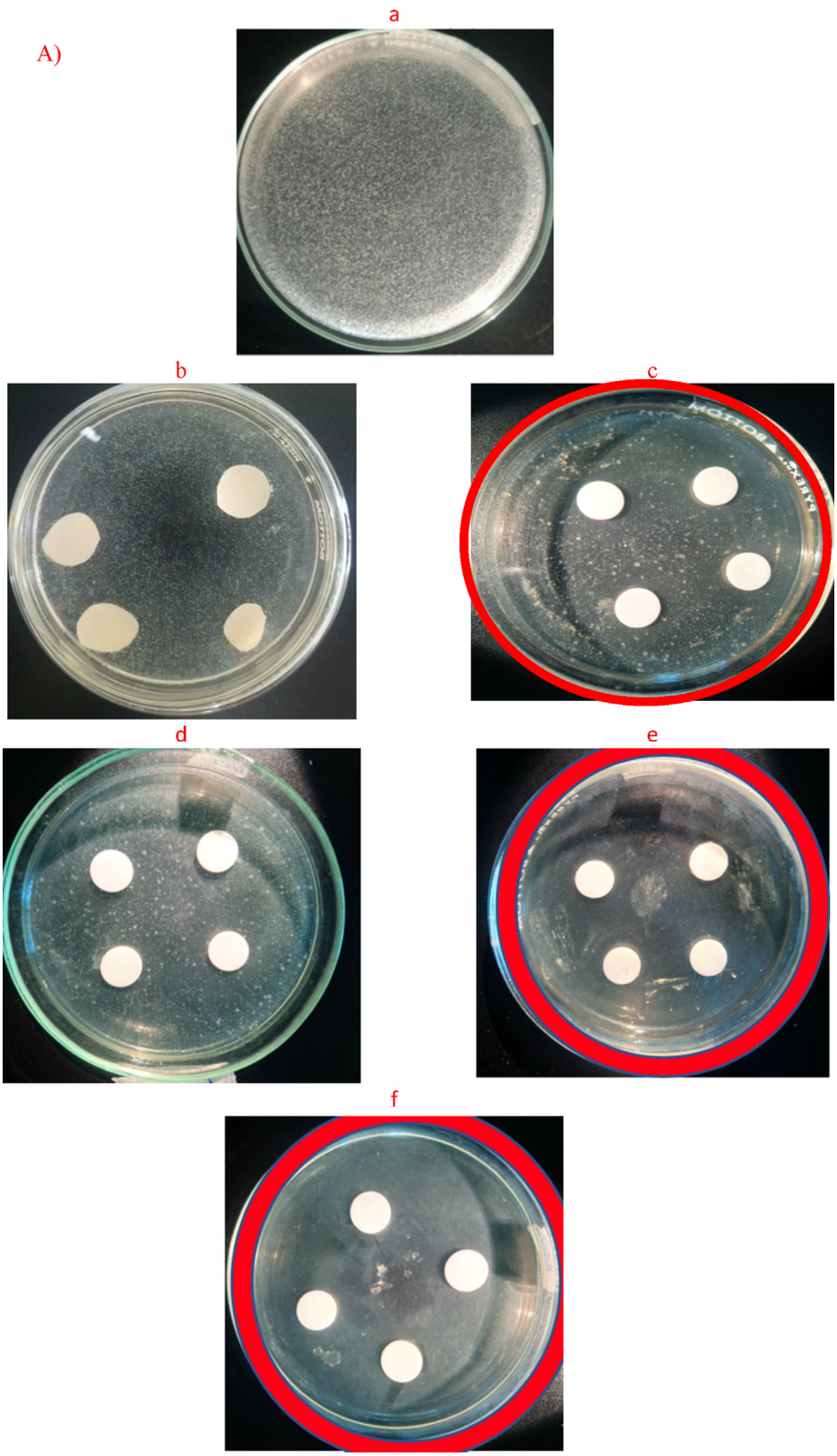

Fig. 9. (A) of inhibitory effect of the Nanoparticles on membrane surface against *B, Subtilis* (a) blank, and Modified membranes by binding method (b) NF-PDA, (c) NF5b., (d) NFX-1b, (e) NFX-2b, (f) NFX-3b, membranes after 30 min of UV irradiation. (B) Quantified antimicrobial ability of the control, NF-PDA, NF5b, NFX1b, NFX-2b and NFX-3b modified membranes by binding method.

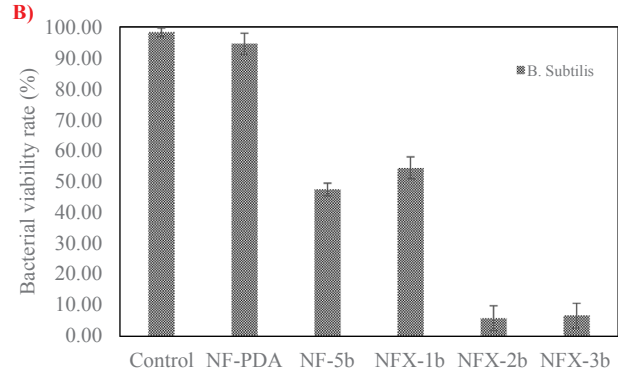

Fig. 9. (*continued*)

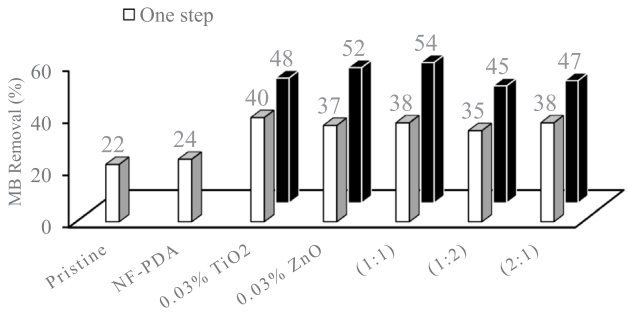

Fig. 10. Degradation of the MB under visible light irradiation as a function of time for the various modified membranes (Co = 10 mg L^{-1}, time of irradiation = 180 min).

3.3. Membrane hydrophilicity

Superhydrophilic or superhydrophobic surfaces are self-cleaning, such as *Nelumbo nucifera* (lotus leaves) and *Ruellia devosiana* [56,57]. In water purification, hydrophilic surfaces are preferred, which can be achieved by changing both surface roughness and free surface energy [34,58]. A change of surface roughness on the membrane surface can be achieved by modifying the surface with PDA or by adding metal oxide nanoparticles on the surface of the membranes [59,60] as in the Section 3.2 and Fig. S2. Adding nanoparticles on the membrane can cause a change in the surface energy of the PDA and hence this can cause the hydrophilicity of the membrane may change, because nanoparticles tend to be attracted to each other through van der Waals forces and the surface of the nanoparticles have a surface energy of their own. In addition, the contribution to the hydrophilicity of the membrane can also be caused to the fact that the oxygen in TiO_2 and ZnO can be bridging or threefold coordinated and then, this oxygen reacts causing vacancies that produce dissociative adsorption of water at the vacancy site [22,61].

Fig. 5 shows the water contact angles of pristine and modified membranes. The pristine membrane had low contact angle, this showed that the membrane had hydrophilic proprieties. For the PDA membrane the contact angle of the membranes is only slightly increased in comparison with the pristine membrane, similar to the work of Zhang et al. [34]. In this case, PDA itself is a hydrophilic material and contains hydrophilic functional groups, such as amines and catechols [62,63]. However, the PDA membrane was not found more hydrophilic than the pristine membrane, this is probably related to a solid-liquid-air interface, formed between the water droplet and the polydopamine surface. The modification of the membrane surface with polydopamine can generate roughness in the membrane (ridges and valleys). When the nanoscale narrow valleys of the polydopamine layer make contact with water droplets, water may not penetrate into the surface cavities, which results in the formation of air pockets and leads to a composite interface [64].

Membranes containing nanoparticles on the PDA-modified membrane surface were more hydrophilic than the pristine and PDA coated membranes.

For the one-step method, membranes modified with PDA and nanoparticles improved the hydrophilicity. This modification caused a decrease in the contact angle value because nanoparticles increased the hydrophilicity. Furthermore, the membrane could be still negatively charged even after the modification. For this reason, the rejection of ions was also high during the nanofiltration tests, as shown in the next section (Fig. 7a).

The membranes modified by the two-step binding method showed a greater hydrophilicity compared to the membranes modified by the one-step co-deposition method, which could be explained by the coating of the surface of metal oxide nanoparticles by polymerization of polydopamine in the co-deposition method [34,58] whereas in the two-step method, a continuous growth of the nanoparticles that bind to the PDA layer allows for a more hydrophilic surface.

3.4. Water permeability

Fig. 6 shows the average water permeability of the pristine membrane and each modified membrane. The pristine membrane achieved a water permeability of 7.2 L $m^{-2}h^{-1}$ bar^{-1}. After PDA layer deposition, the water permeability dropped to 6.1 L $m^{-2}h^{-1}$ bar^{-1}. This decrease represents the surface structure of the polydopamine film *via* $CuSO_4$/H_2O_2-triggered fast PDA deposition [24]. Interestingly, co-deposition membranes coated with TiO_2 nanoparticles (0.01%, 0.03% and 0.05%) achieved a higher permeability in comparison with the PDA modified membrane: from 6.3 to 6.8, 7.7 and 7.8 L $m^{-2}h^{-1}$ bar^{-1}, respectively. However, the membranes coated with ZnO nanoparticles (0.01% and 0.05%) showed a decrease in permeability compared with membranes with PDA coating, while the membrane with ZnO nanoparticles (0.03%) showed an increase in permeability to 7.1 L $m^{-2}h^{-1}$ bar^{-1}.

For two-step coating, the water permeability progressively decreases from 6.8 to 6.2 and 5.9 L $m^{-2}h^{-1}$ bar^{-1} by increasing TiO_2 nanoparticles concentration to 0.01%, 0.03% and 0.05% respectively. ZnO nanoparticles had a similar behavior. This is ascribed to the strong binding of nanoparticles via electrostatic attraction into the membrane surface pores. This suggests that PDA functionalization is a process that depends on the concentration of nanoparticles: a higher concentration of nanoparticles leads to a denser membrane.

Thus, TiO_2 nanoparticles yield a higher water permeability in comparison with ZnO nanoparticles by the co-deposition method. In addition, the increase in nanoparticles concentration on the surface membranes in the two-step method increases the hydraulic resistance, slightly decreasing the water permeability.

For the nanoparticles mixture (TiO_2:ZnO) applied in the co-deposition and binding methods, all the prepared membranes by both methods showed a lower permeability than the pristine membrane. At the same time, Fig. 6, also shows that the water permeability improved when the concentration of ZnO nanoparticles is higher than the concentration TiO_2 nanoparticles by the co-deposition method. This may be because the catalysts (TiO_2:ZnO) compete for binding sites on the membrane surface; ZnO does not have a very strong bond with the PDA surface because it has only one oxygen in its structure to form a complex with the PDA. Therefore, when the concentration of ZnO nanoparticles increases compared to TiO_2, the same permeability is reached as the membrane coated only with PDA since the nanoparticles are not strongly attached to the membrane surface. This is confirmed by SEM images (Fig. S2).

For the two-step method, the increase in the ratio of ZnO nanoparticles in the nanoparticles mixture decreases the water permeability. This decrease suggests a strong coating of TiO_2 nanoparticles and a fragile coating of ZnO nanoparticles onto the PDA layer. This could be because TiO_2 has more oxygen atoms in its molecule and these atoms

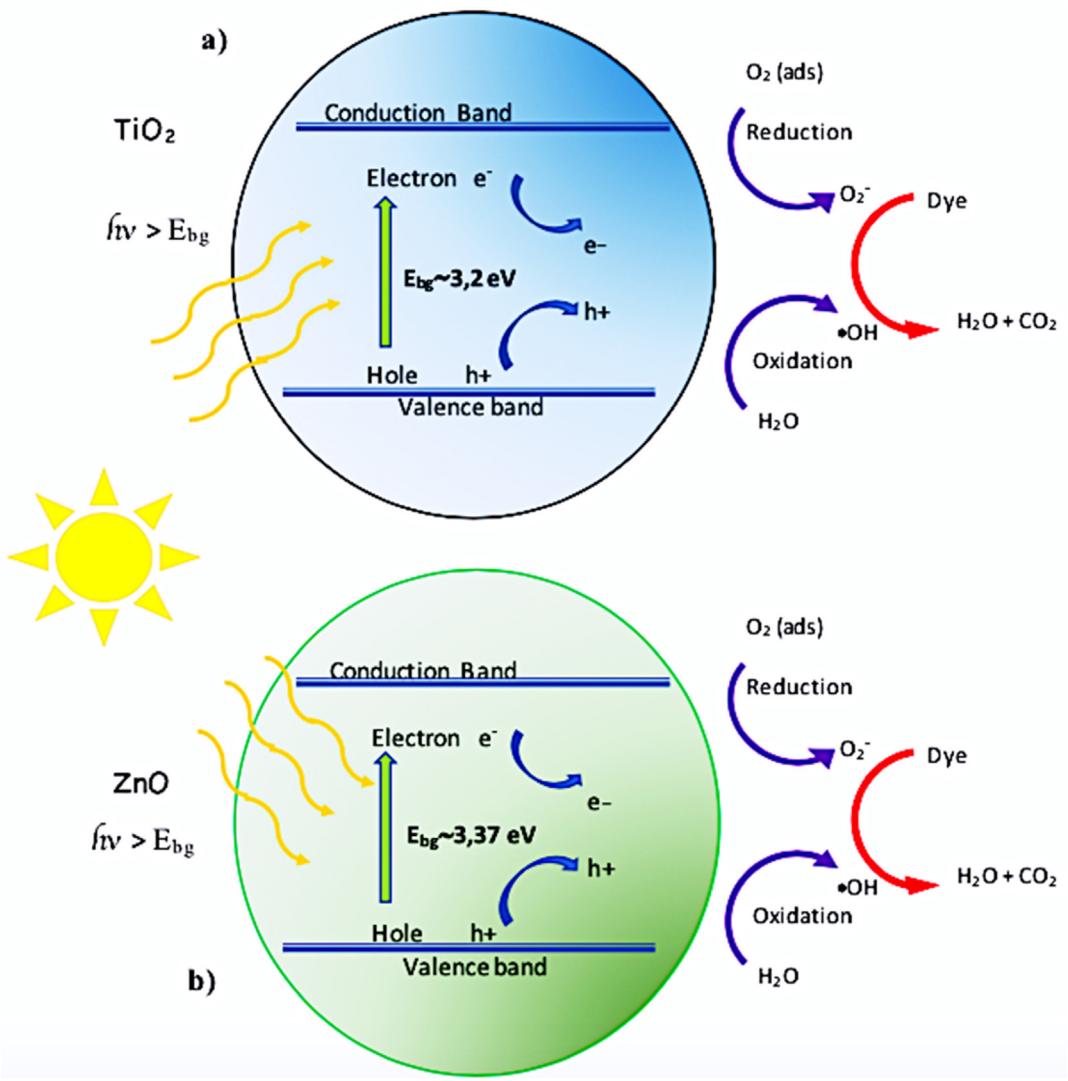

Fig. 11. Mechanism of photodegradation of dyes using TiO_2 and ZnO [88].

are threefold coordinated with the PDA surface [22,61]. The greater amount of TiO_2 nanoparticles on the PDA surface generates a higher roughness on the membrane surface and improves permeability. Previous work has reported that an increased membrane roughness can improve the permeability. The low compatibility of inorganic and polymer materials can create a narrow gap around the inorganic particles that increases the flux [65]. Overall, membranes modified with TiO_2 have a more favorable effect on water permeability than ZnO. This effect is similar when there is a higher proportion of TiO_2 in the catalyst mixture for two-step modification.

3.5. Separation properties of NF membranes

The NF performance of the membranes was systematically evaluated by individually testing the retentions of two salts ($MgSO_4$ and NaCl) at 4 bar, inlet concentrations of 1.0 g L^{-1}. Fig. 7 compares the salt rejections of membranes with different ratios of catalysts (TiO_2 and ZnO). The membranes modified by co-deposition and binding methods exhibited a slight increase NaCl rejection, probably due to the nanoparticles and nanosized polydopamine oligomers that may block or grow in the defects or larger pores of the pristine membrane surfaces at the early stage.

Furthermore, considering the rejection range and the standard deviation, there seems to be no significant difference in salt rejections for the membranes modified by a combination of TiO_2:ZnO using both binding methods.

The modification of membranes with a PDA layer and nanoparticle deposition by co-deposition and two-step method does not appear to have a significant influence on the $MgSO_4$ rejection ~95% (Fig. 7). The membranes maintain the excellent properties of the pristine membrane.

3.6. Anti-bacterial activity of modified membranes

3.6.1. Iso Sensitest

The antibacterial activity of the modified NF membranes was evaluated by observing the growth rate of nine specific seeding plates containing *Bacillus subtilis*, irradiated with UV [45].

As shown in Fig. S4 and Fig. 8, the co-deposition method showed no inhibition. This may be due to the fact that in the co-deposition method the catalyst nanoparticles may have been coated by a PDA layer.

For the binding method (two steps), the exposure of the membranes to the UV light effectively decreased the viability of the *Bacillus subtilis* for the membrane with 0.03%wt (ZnO) (Fig. 8b). The membrane with 0.03% TiO_2 exhibited no inhibition for *Bacillus subtilis*.

The antibacterial effect of ZnO nanoparticles may be due to the cell wall structure of Gram-positive bacteria. More precisely, the Gram-positive cell wall consists of a peptidoglycan layer that is bound to teichoic acids, which should be in close proximity with ZnO

nanoparticles to create oxidative stress on bacteria resulting in antibacterial activity. There are reports indicating that nanomaterials as ZnO can be adsorbed on the bacterial surface, interacting with bacteria [66,67].

Derjaguin-Landau-Verwey-Overbeek (DLVO) theory says that the interaction energy between bacteria and a metal oxide can be due to three components, apolar van der Waals forces, electrostatic and polar Lewis acid base component [68]. In addition, MacLean et al. [69] studied adsorption of compounds on a bacterial surface through reactive positive sites derived from amino functional groups of peptidoglycan and proteins associated with the cell wall. Therefore, materials like ZnO nanoparticles can be absorbed on the surface of the bacteria, resulting in antibacterial activity. On the other hand, the ZnO nanoparticles under UV light irradiation generate free electrons that interact with oxygen, forming superoxides, while the holes convert hydroxyl ions into highly reactive hydroxyl radical ($^{\cdot}OH$). These reactive oxygen species (ROS) damage microbial cell walls, resulting in their inactivation [70]. In addition to this, small amounts of ZnO nanoparticles can slowly dissociate and release Zn^{+2} ions, therefore, Zn^{+2} ions can penetrate through the cell wall of bacteria after that the reactive oxygen species (ROS) damages microbial cell walls to destroy DNA and cytoplasm of bacteria [66]. In consequence, the bactericidal effect of the ZnO on *B. Subtilis* may be due to its soft cell wall as well as higher penetration and destruction capability of Zn^{+2} for Gram-positive bacteria [46,71–73]. The greater inhibition in the presence of light supports the notion that the The higher bactericidal effect of ZnO on B. subtilis could be due to the higher capacity of penetration and destruction of the Zn^{2+} ion to the cell wall of these Gram-positive bacteria, since they have a soft cell wall compared to Gram-negative ones. Although it is not clear why zinc exhibits different bacterial affinity with gram-positive, it may be ascribed to the difference in the protein constituents of their cell walls, [74] In addition, it has been suggested that zinc binds to the membranes of microorganisms, prolonging the lag phase of the growth cycle and increasing the generation time of the organisms so that it takes each of them longer to complete cell division [71,72,75–77]. This property could be beneficial for biofouling mitigation.

3.6.2. Disk diffusion technique

The bactericidal property of the novel membranes against *B. subtilis* was also evaluated using the disk diffusion technique proposed by Lashkenari et al. [46]. In this method, the inhibition zone around the disk shows the antibacterial effect of the membrane.

Fig. 9 shows that the *B. Subtilis* grew at the edge of the modified membranes by the co-deposition method and no obvious inhibition zone are observed in their vicinity (Fig. S5). On the other hand, in membranes synthetized by the two-step method, an inhibition zone is created around the ZnO nanoparticles (0.03 wt%) membrane disk (Fig. 9Ac). Therefore, the membrane with ZnO nanoparticles has a better antibacterial effect in comparison to the membrane with TiO_2 nanoparticles. The mechanism of the biocidal action of ZnO based materials is based on the generation of surface oxygen species, killing the pathogens [66,73,78].

The combination of TiO_2: ZnO (1:2, 2:1) (Fig. 9A e and f) has good activity against *B. Subtilis*. The inhibition zone size is based on the ratio of catalysts. The efficiency of different catalyst ratios has been reported for solid (TiO_2:ZnO) mixtures in aqueous solutions [46,70,79,80]. However, this study presents the first evidences of antibacterial activity in membranes modified with PDA and different compositions of catalysts (TiO_2:ZnO).

In addition, Talebian et al. 2013 [81] demonstrated that the antibacterial activity of ZnO Nanoparticles also depends on the morphology of the Nanoparticles. Future work will investigate how this morphology acts on the surface of modified membranes.

Fig. 9 describes the strong antimicrobial activities of the modified membranes. To quantitatively analyze the bactericidal ability, the viable cell counting technique was applied in this study. The NF-PDA membrane prepared by the fast PDA deposition exhibited a slight antibacterial ability against *B. Subtilis*. This trait may be attributed to the release of copper ions from the PDA layer [24]. Relative to the control sample, the modified membranes reduced 93.0%, 92.7%, 64.7% and 47.5% of *B. Subtilis* when ratios (TiO_2:ZnO 0,03%wt) 2:1, 1:2, 0,03%wt ZnO, and 1:1 binding modification method were applied, respectively (Fig. 9B). Such distinct reductions in *B. Subtilis* colonies demonstrate the excellent antimicrobial properties of the modified membranes.

3.7. Effect of solar light irradiation on membrane surface in degradation of methylene blue

Fig. 10 shows that the membranes can photocatalytically remove dyes from a bulk solution. It should be noted that the methylene blue in the unmodified membrane (pristine) has approximately 20% MB removal. This is because the MB can suffer photolysis by solar irradiation as shown in other reports [82,83].

For modified membranes, the binding method (two-step modification) is more effective in removing dyes from the solution in contact with the membrane in comparison with the co-deposition method (one-step modification method). This could be because the catalysts nanoparticles in the two-step modification method are exposed on the membrane surface directly receiving sun radiation [32,84,85]. Furthermore, a catalyst mixture of 1:1 and 2:1 (TiO_2:ZnO) was found effective for the removal of dyes for aqueous heterogeneous photocatalytic processes [86,87]. This is not the case with one-step modification since co-polymerization could encapsulate the catalyst nanoparticles with a PDA layer and this would reduce the passage of light to the catalysts, decreasing their ability to remove dyes.

Thus, nanoparticles (ZnO, TiO_2, and their mixtures) on the surface of a PDA modified membrane can be potentially used as anti-fouling agents under visible light, following the mechanisms proposed by Prasannalakshmi and Shanmugam for mixing of powders (catalysts) [88] (Fig. 11). The observed photocatalytic activity is exactly matched with the reported results [89–91]. It is important to note that, previous reports have shown photocatalytic activity (under solar irradiation) for the powder ratios of the two catalysts (TIO_2: ZnO), but, no data are available for catalyst ratios on PDA-modified membranes.

The mechanism of the Fig. 11 has been proposed by Prasannalakshmi and Shanmugam for mixing of powders [88].

In the mechanism proposed (under sunlight irradiation), the electrons from the conduction band (CB) of ZnO are transferred to CB of TiO_2. In the same way, the holes are transferred from the valence band (VB) of TiO_2 to VB of ZnO. This process prevents the recombination of charge carriers and makes their availability on the surface of the photocatalysts and thus enhances the redox process (Fig. 11). The high surface area of TiO_2:ZnO accompanies with the optimum pore size and pore volume provides much surface for the absorption of dye molecules which increases the probability of degradation. In addition to this elongated one dimension of ratios of TiO_2:ZnO helps to decrease the recombination probability of photogenerated carriers due to an increased delocalization of electrons [88]. In the present work, we propose this mechanism on the surface of the modified membrane.

In order to demonstrate the efficiency of our modified membranes, figure SS1 shows the two-step modified membranes after being in contact for 5 h with methylene blue solution (10 mg L^{-1}) and under solar irradiation, the membranes by two steps showed much cleaner surfaces after use. This may be due to a synergy between the catalysts, as explained in the previous section. The proposed mechanism for mixing catalysts could be carried out on these modified membranes.

Two preparation techniques were tested: codeposition and two-step deposition of PDA and Catalysts (TiO2 and ZnO). In both cases, PDA deposited rapidly onto a NF support. The two-step modified membranes showed greater antifouling properties than the one-step method when the membranes were in contact with dye solutions. The most optimal

modification method for the antibacterial activity was PDA and nanoparticles by two-step deposition method. Remarkably, modified membranes with ZnO and ratios of catalysts (TiO_2: ZnO) 1:2 and 2:1 have shown high antibacterial activity achieved. The membranes used in this study provide a competitive alternative and practical solution for antifouling applications in nanofiltration. More importantly, this facile two-step deposition strategy offers possibilities in the strong binding of other ratios pf nanoparticles (i.e., Ag, and graphene oxide) with enhanced antimicrobial properties onto the membrane surface

4. Conclusions

In this study, nanoparticles of TiO_2, ZnO and their mixtures were successfully attached to a PDA layer surface of a nanofiltration membrane, by two methods; (1) co-deposition and (2) binding. SEM, EDX, and water contact angle measurements confirmed the formation of a thin hydrophilic PDA layer on the NF membrane surface with homogeneously dispersed structures.

The membranes obtained by the binding method with modifications of 0.03%wt ZnO nanoparticles and a mixture of catalyst TiO_2: ZnO (1:2 and 2:1) showed antibacterial activity against *Bacillus subtilis*. Furthermore, the combination of TiO_2:ZnO catalysts by the binding method may to be used as a practical anti-biofouling nanomaterial. Finally, the combination of TiO_2 nanoparticles with ZnO nanoparticles enhanced the photocatalytic activity of the modified membranes to remove dyes from solution.

CRediT authorship contribution statement

Raúl Bahamonde Soria: Conceptualization, Methodology, Validation, Investigation, Writing - original draft, Writing - review & editing, Visualization. **Junyong Zhu:** Resources, Conceptualization, Validation, Formal analysis, Data curation. **Irma Gonza:** Resources, Conceptualization, Formal analysis, Data curation. **Bart Van der Bruggen:** Validation, Supervision, Writing - review & editing. **Patricia Luis:** Validation, Supervision, Writing - review & editing, Project administration, Funding acquisition.

Declaration of Competing Interest

The authors declare that they have no known competing financial interests or personal relationships that could have appeared to influence the work reported in this paper.

Acknowledgements

The authors acknowledge the support provided by I´Académie de Recherche et d´Enseignemetn Supérieur (ARES) and Central University of Ecuador for financially supporting this work (RFCQ-CQ-SO13-186-2017). The authors greatly thanks Laurence Ryelandt from pole Materials and Processes Engineering (IMAP) UCLouvain, for the SEM and EDX measurements.

Appendix A. Supplementary material

Supplementary data to this article can be found online at https://doi.org/10.1016/j.seppur.2020.117280.

References

[1] C. Bellona, J.E. Drewes, P. Xu, G. Amy, Factors affecting the rejection of organic solutes during NF/RO treatment - A literature review, Water Res. 38 (2004) 2795–2809, https://doi.org/10.1016/j.watres.2004.03.034.
[2] A.W. Mohammad, N. Ali, Understanding the steric and charge contributions in NF membranes using increasing MWCO polyamide membranes, Desalination 147 (2002) 205–212, https://doi.org/10.1016/S0011-9164(02)00535-0.
[3] F. Fu, Q. Wang, Removal of heavy metal ions from wastewaters: a review, J. Environ. Manage. 92 (2011) 407–418, https://doi.org/10.1016/j.jenvman.2010.11.011.
[4] E.M. Vrijenhoek, S. Hong, M. Elimelech, Influence of membrane properties, solution chemistry, and hydrodynamics on colloidal fouling of reverse osmosis and nanofiltration membranes, J. Memb. Sci. 188 (2001) 115–128.
[5] K.C. Khulbe, T. Matsuura, Characterization of synthetic membranes by Raman spectroscopy, electron spin resonance, and atomic force microscopy; a review, Polymer (Guildf). 41 (2000) 1917–1935, https://doi.org/10.1016/S0032-3861(99)00359-6.
[6] H. Ivnitsky, D. Minz, L. Kautsky, A. Preis, A. Ostfeld, R. Semiat, C.G. Dosoretz, Biofouling formation and modeling in nanofiltration membranes applied to wastewater treatment, J. Memb. Sci. 360 (2010) 165–173, https://doi.org/10.1016/j.memsci.2010.05.007.
[7] H. Ivnitsky, I. Katz, D. Minz, E. Shimoni, Y. Chen, J. Tarchitzky, R. Semiat, C.G. Dosoretz, Characterization of membrane biofouling in nanofiltration processes of wastewater treatment, Desalination 185 (2005) 255–268, https://doi.org/10.1016/j.desal.2005.03.081.
[8] R.R. Choudhury, J.M. Gohil, S. Mohanty, S.K. Nayak, Antifouling, fouling release and antimicrobial materials for surface modification of reverse osmosis and nanofiltration membranes, J. Mater. Chem. A 6 (2018) 313–333, https://doi.org/10.1039/c7ta08627j.
[9] H.S. Abid, D.J. Johnson, R. Hashaikeh, N. Hilal, A review of efforts to reduce membrane fouling by control of feed spacer characteristics, Desalination 420 (2017) 384–402, https://doi.org/10.1016/j.desal.2017.07.019.
[10] Y.H. Ding, M. Floren, W. Tan, Mussel-inspired polydopamine for bio-surface functionalization, Biosurface Biotribol. 2 (2016) 121–136, https://doi.org/10.1016/j.bsbt.2016.11.001.
[11] H. Karkhanechi, R. Takagi, H. Matsuyama, Enhanced antibiofouling of RO membranes via polydopamine coating and polyzwitterion immobilization, Desalination 337 (2014) 23–30, https://doi.org/10.1016/j.desal.2014.01.007.
[12] T.F. Wu, J.D. Hong, Dopamine-melanin nanofilms for biomimetic structural coloration, Biomacromolecules 16 (2015) 660–666, https://doi.org/10.1021/bm501773c.
[13] S. Kasemset, A. Lee, D.J. Miller, B.D. Freeman, M.M. Sharma, Effect of polydopamine deposition conditions on fouling resistance, physical properties, and permeation properties of reverse osmosis membranes in oil/water separation, J. Memb. Sci. 425–426 (2013) 208–216, https://doi.org/10.1016/j.memsci.2012.08.049.
[14] K.Y. Kim, E. Yang, M.Y. Lee, K.J. Chae, C.M. Kim, I.S. Kim, Polydopamine coating effects on ultrafiltration membrane to enhance power density and mitigate biofouling of ultrafiltration microbial fuel cells (UF-MFCs), Water Res. 54 (2014) 62–68, https://doi.org/10.1016/j.watres.2014.01.045.
[15] Y. Xiang, F. Liu, L. Xue, Under seawater superoleophobic PVDF membrane inspired by polydopamine for efficient oil/seawater separation, Elsevier, 2015. doi: 10.1016/j.memsci.2014.11.052.
[16] M. Vaselbehagh, H. Karkhanechi, S. Mulyati, R. Takagi, H. Matsuyama, Improved antifouling of anion-exchange membrane by polydopamine coating in electrodialysis process, Desalination 332 (2014) 126–133, https://doi.org/10.1016/j.desal.2013.10.031.
[17] L. Liu, B. Shao, F. Yang, Polydopamine coating - Surface modification of polyester filter and fouling reduction, Sep. Purif. Technol. 118 (2013) 226–233, https://doi.org/10.1016/j.seppur.2013.07.003.
[18] M.H. Ryou, D.J. Lee, J.N. Lee, Y.M. Lee, J.K. Park, J.W. Choi, Excellent cycle life of lithium-metal anodes in lithium-ion batteries with mussel-inspired polydopamine-coated separators, Adv. Energy Mater. 2 (2012) 645–650, https://doi.org/10.1002/aenm.201100687.
[19] T.G. Barclay, H.M. Hegab, S.R. Clarke, M. Ginic-Markovic, Versatile surface modification using polydopamine and related polycatecholamines: chemistry, structure, and applications, Adv. Mater. Interfaces. 4 (2017) 1–38, https://doi.org/10.1002/admi.201601192.
[20] D.J. Miller, P.A. Araújo, P.B. Correia, M.M. Ramsey, J.C. Kruithof, M.C.M. van Loosdrecht, B.D. Freeman, D.R. Paul, M. Whiteley, J.S. Vrouwenvelder, Short-term adhesion and long-term biofouling testing of polydopamine and poly(ethylene glycol) surface modifications of membranes and feed spacers for biofouling control, Water Res. 46 (2012) 3737–3753, https://doi.org/10.1016/j.watres.2012.03.058.
[21] D.J. Miller, S. Kasemset, L. Wang, D.R. Paul, B.D. Freeman, Constant flux crossflow filtration evaluation of surface-modified fouling-resistant membranes, J. Memb. Sci. 452 (2014) 171–183, https://doi.org/10.1016/j.memsci.2013.10.037.
[22] H. Lee, S.M. Dellatore, W.M. Miller, P.B. Messersmith, Mussel-inspired surface chemistry for multifunctional coatings, Science (80-.) 318 (2007) 426–430. doi: 10.1126/science.1147241.Mussel-Inspired.
[23] C. Zhang, H.N. Li, Y. Du, M.Q. Ma, Z.K. Xu, CuSO4/H2O2-Triggered polydopamine/poly(sulfobetaine methacrylate) coatings for antifouling membrane surfaces, Langmuir 33 (2017) 1210–1216, https://doi.org/10.1021/acs.langmuir.6b03948.
[24] J. Zhu, A. Uliana, J. Wang, S. Yuan, J. Li, M. Tian, K. Simoens, A. Volodin, J. Lin, K. Bernaerts, Y. Zhang, B. Van Der Bruggen, Elevated salt transport of antimicrobial loose nanofiltration membranes enabled by copper nanoparticles: Via fast bioinspired deposition, J. Mater. Chem. A. 4 (2016) 13211–13222, https://doi.org/10.1039/c6ta05661j.
[25] A.W. Mohammad, Y.H. Teow, W.L. Ang, Y.T. Chung, D.L. Oatley-Radcliffe, N. Hilal, Nanofiltration membranes review: recent advances and future prospects, Desalination 356 (2015) 226–254.
[26] L.Y. Ng, A.W. Mohammad, C.P. Leo, N. Hilal, Polymeric membranes incorporated with metal/metal oxide nanoparticles: A comprehensive review, Desalination 308 (2013) 15–33, https://doi.org/10.1016/j.desal.2010.11.033.
[27] M. Homayoonfal, M.R. Mehrnia, Y.M. Mojtahedi, A.F. Ismail, Effect of metal and

metal oxide nanoparticle impregnation route on structure and liquid filtration performance of polymeric nanocomposite membranes: A comprehensive review, Desalin. Water Treat. 51 (2013) 3295–3316, https://doi.org/10.1080/19443994.2012.749055.
[28] T. Rajh, L.X. Chen, K. Lukas, T. Liu, M.C. Thurnauer, D.M. Tiede, Surface restructuring of nanoparticles: An efficient route for ligand-metal oxide crosstalk, J. Phys. Chem. B. 106 (2002) 10543–10552, https://doi.org/10.1021/jp021235v.
[29] J.L. Dalsin, L. Lin, S. Tosatti, J. Vo, M. Textor, P.B. Messersmith, Protein resistance of titanium oxide surfaces modified by biologically inspired mPEG - DOPA, Langmuir 21 (2005) 640–646.
[30] M. Rodenstein, S. Zürcher, S.G.P. Tosatti, N.D. Spencer, Fabricating chemical gradients on oxide surfaces by means of fluorinated, catechol-based, self-assembled monolayers, Langmuir 26 (2010) 16211–16220, https://doi.org/10.1021/la100805z.
[31] Q. Ye, F. Zhou, W. Liu, Bioinspired catecholic chemistry for surface modification, Chem. Soc. Rev. 40 (2011) 4244–4258, https://doi.org/10.1039/c1cs15026j.
[32] G. De Filpo, E. Pantuso, K. Armentano, P. Formoso, G. Di Profio, T. Poerio, E. Fontananova, C. Meringolo, A.I. Mashin, F.P. Nicoletta, Chemical vapor deposition of photocatalyst nanoparticles on PVDF membranes for advanced oxidation processes, Membranes (Basel). 8 (2018) 35, https://doi.org/10.3390/membranes8030035.
[33] H.C. Yang, K.J. Liao, H. Huang, Q.Y. Wu, L.S. Wan, Z.K. Xu, Mussel-inspired modification of a polymer membrane for ultra-high water permeability and oil-in-water emulsion separation, J. Mater. Chem. A. 2 (2014) 10225, https://doi.org/10.1039/c4ta00143e.
[34] R.-X. Zhang, L. Braeken, T. Liu, P. Luis, X.-L. Wang, B. Van der Bruggen, Remarkable Anti-Fouling performance of TiO2-modified TFC membranes with mussel-inspired polydopamine binding, Appl. Sci. 7 (2017) 81.
[35] R.X. Zhang, L. Braeken, P. Luis, X.L. Wang, B. Van der Bruggen, Novel binding procedure of TiO2 nanoparticles to thin film composite membranes via self-polymerized polydopamine, J. Memb. Sci. 437 (2013) 179–188, https://doi.org/10.1016/j.memsci.2013.02.059.
[36] J. Zhu, S. Yuan, A. Uliana, J. Hou, J. Li, X. Li, M. Tian, Y. Chen, A. Volodin, B. Van Der Bruggen, High- flux thin film composite membranes for nano filtration mediated by a rapid co-deposition of polydopamine / piperazine, J. Memb. Sci. 554 (2018) 97–108, https://doi.org/10.1016/j.memsci.2018.03.004.
[37] S.R. Lakhotia, M. Mukhopadhyay, P. Kumari, Iron oxide (FeO) nanoparticles embedded thin-film nanocomposite T nanofiltration (NF) membrane for water treatment, 211 (2019) 98–107.
[38] Z. Yang, Y. Wu, J. Wang, B. Cao, C.Y. Tang, In situ reduction of silver by polydopamine: A novel antimicrobial modification of a thin-film composite polyamide membrane, Environ. Sci. Technol. 50 (2016) 9543–9550, https://doi.org/10.1021/acs.est.6b01867.
[39] P. Lu, S. Liang, T. Zhou, T. Xue, X. Mei, Q. Wang, Layered double hydroxide nanoparticle modified forward osmosis membranes via polydopamine immobilization with significantly enhanced chlorine and fouling resistance, Desalination. 421 (2017) 99–109, https://doi.org/10.1016/j.desal.2017.04.030.
[40] J.H. Kim, C.H. Park, C.S. Kim, M.K. Joshi, J. Lee, Polydopamine-assisted immobilization of hierarchical zinc oxide nanostructures on electrospun nanofibrous membrane for photocatalysis and antimicrobial activity, J. Colloid Interface Sci. 513 (2017) 566–574, https://doi.org/10.1016/j.jcis.2017.11.061.
[41] N. Noshirvani, B. Ghanbarzadeh, M. Reza, M. Hashemi, V. Coma, Preparation and characterization of active emulsified films based on chitosan-carboxymethyl cellulose containing zinc oxide nano particles, Int. J. Biol. Macromol. 99 (2017) 530–538 doi: 1037//0033-2909.I26.1.78.
[42] M. Peyravi, M. Jahanshahi, A. Rahimpour, A. Javadi, S. Hajavi, Novel thin film nanocomposite membranes incorporated with functionalized TiO2 nanoparticles for organic solvent nanofiltration, Chem. Eng. J. 241 (2014) 155–166, https://doi.org/10.1016/j.cej.2013.12.024.
[43] X. Zhao, Y. Su, Y. Liu, R. Zhang, Z. Jiang, Multiple antifouling capacities of hybrid membranes derived from multifunctional titania nanoparticles, J. Memb. Sci. 495 (2015) 226–234, https://doi.org/10.1016/j.memsci.2015.08.026.
[44] J. Zhu, M. Tilahun, J. Wang, A. Uliana, M. Tian, S. Yuan, J. Li, Y. Zhang, A. Volodin, B. Van Der Bruggen, A rapid deposition of polydopamine coatings induced by iron (III) chloride / hydrogen peroxide for loose nanofiltration, J. Colloid Interface Sci. 523 (2018) 86–97, https://doi.org/10.1016/j.jcis.2018.03.072.
[45] B. Khorshidi, I. Biswas, T. Ghosh, T. Thundat, M. Sadrzadeh, Robust fabrication of thin film polyamide-TiO2 nanocomposite membranes with enhanced thermal stability and anti-biofouling propensity, Sci. Rep. 8 (2018) 784, https://doi.org/10.1038/s41598-017-18724-w.
[46] A. Soleymani Lashkenari, M.T. Hamed Mosavian, M. Peyravi, M. Jahanshahi, Biofouling mitigation of bilayer polysulfone membrane assisted by zinc oxide-polyrhodanine couple nanoparticle, Prog. Org. Coatings. 129 (2019) 147–158, https://doi.org/10.1016/j.porgcoat.2018.12.012.
[47] Q.E. Ambient Secretary, Ambient secretary government of Quito Ecuador, 2018. http://www.quitoambiente.gob.ec/ambiente/index.php/radiacion-ultravioleta-app.
[48] D. Rajamanickam, M. Shanthi, Photocatalytic degradation of an organic pollutant, 4-nitrophenol by zinc oxide - UV process, Res. J. Chem. Environ. 9 (2012) S1858–S1868.
[49] S. Hong, Y.S. Na, S. Choi, I.T. Song, W.Y. Kim, H. Lee, Non-covalent self-assembly and covalent polymerization co-contribute to polydopamine formation, Adv. Funct. Mater. 22 (2012) 4711–4717, https://doi.org/10.1002/adfm.201201156.
[50] V. Ball, Polydopamine films and particles with catalytic activity, Catal. Today. 301 (2018) 196–203, https://doi.org/10.1016/j.cattod.2017.01.031.
[51] Z. Liu, Y. Hu, C. Liu, Z. Zhou, Surface-independent one-pot chelation of copper ions onto filtration membranes to provide antibacterial properties, Chem. Commun. 52 (2016) 12245–12248, https://doi.org/10.1039/c6cc06015c.
[52] F. Bernsmann, V. Ball, F. Addiego, A. Ponche, M. Michel, J.J. de A. Gracio, V. Toniazzo, D. Ruch, Dopamine−Melanin film deposition depends on the used oxidant and buffer solution, Langmuir 27 (2011) 2819–2825. doi: 10.1021/la104981s.
[53] M. Guvendiren, P.B. Messersmith, K.R. Shull, Self-assembly and adhesion of DOPA-modified methacrylic triblock hydrogels, Biomacromolecules 9 (2008) 122–128, https://doi.org/10.1021/bm700886b.
[54] J. Ran, M. He, W. Li, D. Cheng, X. Wang, Growing ZnO nanoparticles on polydopamine-templated cotton fabrics for durable antimicrobial activity and UV protection, Polymers (Basel) 10 (2018) 495, https://doi.org/10.3390/polym10050495.
[55] J. Ou, J. Wang, D. Zhang, P. Zhang, S. Liu, P. Yan, B. Liu, S. Yang, Fabrication and biocompatibility investigation of TiO 2 films on the polymer substrates obtained via a novel and versatile route, Colloids Surfaces B Biointerfaces 76 (2010) 123–127, https://doi.org/10.1016/j.colsurfb.2009.10.024.
[56] K. Koch, W. Barthlott, Superhydrophobic and superhydrophilic plant surfaces: An inspiration for biomimetic materials, Philos. Trans. R. Soc. A Math. Phys. Eng. Sci. 367 (2009) 1487–1509, https://doi.org/10.1098/rsta.2009.0022.
[57] J. Cui, Z. Zhou, A. Xie, M. Meng, Y. Cui, S. Liu, J. Lu, S. Zhou, Y. Yan, H. Dong, Bio-inspired fabrication of superhydrophilic nanocomposite membrane based on surface modification of SiO2 anchored by polydopamine towards effective oil-water emulsions separation, Sep. Purif. Technol. 209 (2019) 434–442, https://doi.org/10.1016/j.seppur.2018.03.054.
[58] S.H. Yun, P.G. Ingole, K.H. Kim, W.K. Choi, J.H. Kim, H.K. Lee, Properties and performances of polymer composite membranes correlated with monomer and polydopamine for flue gas dehydration by water vapor permeation, Chem. Eng. J. 258 (2014) 348–356, https://doi.org/10.1016/j.cej.2014.07.038.
[59] J. Mansouri, S. Harrisson, V. Chen, Strategies for controlling biofouling in membrane filtration systems: Challenges and opportunities, J. Mater. Chem. 20 (2010) 4567–4586, https://doi.org/10.1039/b926440j.
[60] A. Sotto, A. Boromand, R. Zhang, P. Luis, J.M. Arsuaga, J. Kim, B. Van der Bruggen, Effect of nanoparticle aggregation at low concentrations of TiO 2 on the hydrophilicity, morphology, and fouling resistance of PES-TiO 2 membranes, J. Colloid Interface Sci. 363 (2011) 540–550, https://doi.org/10.1016/j.jcis.2011.07.089.
[61] T. Watanabe, A. Nakajima, R. Wang, M. Minabe, S. Koizumi, A. Fujishima, K. Hashimoto, Photocatalytic activity and photoinduced hydrophilicity of titanium dioxide coated glass, Thin Solid Films. 351 (1999) 260–263, https://doi.org/10.1016/s0040-6090(99)00205-9.
[62] M.B.M.Y. Ang, C.A. Trilles, M.R. De Guzman, J.M. Pereira, R.R. Aquino, S.H. Huang, C.C. Hu, K.R. Lee, J.Y. Lai, Improved performance of thin-film nanocomposite nanofiltration membranes as induced by embedded polydopamine-coated silica nanoparticles, Sep. Purif. Technol. 224 (2019) 113–120, https://doi.org/10.1016/j.seppur.2019.05.018.
[63] H. Zangeneh, A. Akbar, S. Zinadini, M. Feyzi, D.W. Bahnemann, A novel photocatalytic self-cleaning PES nano fi ltration membrane incorporating triple metal-nonmetal doped TiO 2 (K-B-N-TiO 2) for post treatment of biologically treated palm oil mill e ffl uent, React. Funct. Polym. 127 (2018) 139–152.
[64] B. Bhushan, Bioinspired structured surfaces, Langmuir 28 (2012) 1698–1714, https://doi.org/10.1021/la2043729.
[65] L.Y. Ng, C.P. Leo, A.W. Mohammad, Optimizing the incorporation of silica nanoparticles in polysulfone/poly(vinyl alcohol) membranes with response surface methodology law, J. Appl. Polym. Sci. 121 (2011) 1804–1814, https://doi.org/10.1002/app.33628.
[66] V. Lakshmi Prasanna, R. Vijayaraghavan, Chemical manipulation of oxygen vacancy and antibacterial activity in ZnO, Mater. Sci. Eng. C. 77 (2017) 1027–1034, https://doi.org/10.1016/j.msec.2017.03.280.
[67] K. Feris, C. Otto, J. Tinker, D. Wingett, A. Punnoose, A. Thurber, M. Kongara, M. Sabetian, B. Quinn, C. Hanna, D. Pink, Electrostatic interactions affect nanoparticle-mediated toxicity to gram-negative bacterium pseudomonas aeruginosa PAO1, Langmuir. 26 (2010) 4429–4436, https://doi.org/10.1021/la903491z.
[68] W. Zhang, B. Rittmann, Y. Chen, Size effects on adsorption of hematite nanoparticles on E. coli cells, Environ. Sci. Technol. 45 (2011) 2172–2178, https://doi.org/10.1021/es103376y.
[69] L.C.W. MacLean, R.E. Martinez, D.A. Fowle, Experimental studies of bacteria-iodide adsorption interactions, Chem. Geol. 212 (2004) 229–238, https://doi.org/10.1016/j.chemgeo.2004.08.014.
[70] W.J. Parak, T. Rojo, K.M. Fromm, I.R. de Larramendi, M.J. Hajipour, M. Mahmoudi, V. Serpooshan, A. Akbar Ashkarran, D. Jimenez de Aberasturi, Antibacterial properties of nanoparticles, Trends Biotechnol. 30 (2012) 499–511, https://doi.org/10.1016/j.tibtech.2012.06.004.
[71] A. Sirelkhatim, S. Mahmud, A. Seeni, N.H.M. Kaus, L.C. Ann, S.K.M. Bakhori, H. Hasan, D. Mohamad, Review on zinc oxide nanoparticles: Antibacterial activity and toxicity mechanism, Nano-Micro Lett. 7 (2015) 219–242, https://doi.org/10.1007/s40820-015-0040-x.
[72] N.H.H. Hairom, A.W. Mohammad, A.A.H. Kadhum, Effect of various zinc oxide nanoparticles in membrane photocatalytic reactor for Congo red dye treatment, Sep. Purif. Technol. 137 (2014) 74–81, https://doi.org/10.1016/j.seppur.2014.09.027.
[73] A. Senthilraja, B. Krishnakumar, R. Hariharan, A.J.F.N. Sobral, C. Surya, N.A.A. John, M. Shanthi, Synthesis and characterization of bimetallic nanocomposite and its photocatalytic, antifungal and antibacterial activity, Sep. Purif. Technol. 202 (2018) 373–384, https://doi.org/10.1016/j.seppur.2018.04.015.
[74] B. Sugarman, Zinc and infection, Rev. Infect. Dis. 5 (1983) 137–147, https://doi.org/10.1093/clinids/5.1.137.
[75] P. Sathe, M.T.Z. Myint, S. Dobretsov, J. Dutta, Removal and regrowth inhibition of

microalgae using visible light photocatalysis with ZnO nanorods: A green technology, Sep. Purif. Technol. 162 (2016) 61–67, https://doi.org/10.1016/j.seppur.2016.02.007.
[76] L. Radke, B. Hahn, D. Wagner, P. Sohnle, Effect of abscess fluid supernatants on the kinetics of Candida albicans growth, Clin. Immunol. Immunopathol. 73 (1994) 344–349.
[77] S. Atmaca, K. Gül, R. Çiçek, The Effect of Zinc On Microbial Growth, Tr. J. Med. Sci. 28 (2998) 595–597.
[78] N. Haghighi, Y. Abdi, F. Haghighi, Light-induced antifungal activity of TiO 2 nanoparticles/ZnO nanowires, Appl. Surf. Sci. 257 (2011) 10096–10100, https://doi.org/10.1016/j.apsusc.2011.06.145.
[79] L.K. Adams, D.Y. Lyon, P.J.J. Alvarez, Comparative eco-toxicity of nanoscale TiO2, SiO2, and ZnO water suspensions, Water Res. 40 (2006) 3527–3532, https://doi.org/10.1016/j.watres.2006.08.004.
[80] F. Yalcinkaya, D. Lubasova, Quantitative evaluation of antibacterial activities of nanoparticles (ZnO, TiO2, ZnO/TiO2, SnO2, CuO, ZrO2, and AgNO3) incorporated into polyvinyl butyral nanofibers, Polym. Adv. Technol. 28 (2017) 137–140, https://doi.org/10.1002/pat.3883.
[81] N. Talebian, S.M. Amininezhad, M. Doudi, Controllable synthesis of ZnO nanoparticles and their morphology-dependent antibacterial and optical properties, J. Photochem. Photobiol. B Biol. 120 (2013) 66–73, https://doi.org/10.1016/j.jphotobiol.2013.01.004.
[82] T. Soltani, M.H. Entezari, Photolysis and photocatalysis of methylene blue by ferrite bismuth nanoparticles under sunlight irradiation, J. Mol. Catal. A Chem. 377 (2013) 197–203, https://doi.org/10.1016/j.molcata.2013.05.004.
[83] M. Rani, U. Shanker, Sun-light driven rapid photocatalytic degradation of methylene blue by poly(methyl methacrylate)/metal oxide nanocomposites, Colloids Surfaces A Physicochem. Eng. Asp. 559 (2018) 136–147, https://doi.org/10.1016/j.colsurfa.2018.09.040.
[84] P. Raizada, P. Singh, A. Kumar, G. Sharma, B. Pare, S.B. Jonnalagadda, P. Thakur, Solar photocatalytic activity of nano-ZnO supported on activatedcarbon or brick grain particles: Role of adsorption in dye degradation, Appl. Catal. A Gen. 486 (2014) 159–169, https://doi.org/10.1016/j.apcata.2014.08.043.
[85] J. Wang, Y. Xie, Z. Zhang, J. Li, X. Chen, L. Zhang, R. Xu, X. Zhang, Photocatalytic degradation of organic dyes with Er3+: YAlO3/ZnO composite under solar light, Sol. Energy Mater. Sol. Cells. 93 (2009) 355–361, https://doi.org/10.1016/j.solmat.2008.11.017.
[86] D. Štrbac, G. Štrbac, C.A. Aggelopoulos, M. Dimitropoulos, M. Novaković, T. Ivetić, S.N. Yannopoulos, Photocatalytic degradation of Naproxen and methylene blue: Comparison between ZnO, TiO 2 and their mixture, Process Saf. Environ. Prot. 113 (2018) 174–183, https://doi.org/10.1016/j.psep.2017.10.007.
[87] S. Moradi, P. Aberoomand-azar, S. Raeis-farshid, S. Abedini-Khorrami, M.H. Givianrad, The effect of different molar ratios of ZnO on characterization and photocatalytic activity of TiO2/ZnO nanocomposite, J. Saudi Chem. Soc. 20 (2016) 373–378.
[88] P. Prasannalakshmi, N. Shanmugam, Fabrication of TiO2/ZnO nanocomposites for solar energy driven photocatalysis, Mater. Sci. Semicond. Process. 61 (2017) 114–124, https://doi.org/10.1016/j.mssp.2017.01.008.
[89] J. Tian, L. Chen, Y. Yin, X. Wang, J. Dai, Z. Zhu, X. Liu, P. Wu, Photocatalyst of TiO2/ZnO nano composite film: Preparation, characterization, and photodegradation activity of methyl orange, Surf. Coatings Technol. 204 (2009) 205–214, https://doi.org/10.1016/j.surfcoat.2009.07.008.
[90] C.M. Firdaus, M.S.B. Shah Rizam, M. Rusop, S. Rahmatul Hidayah, Characterization of ZnO and ZnO: TiO2 thin films prepared by sol-gel spray-spin coating technique, Procedia Eng. 41 (2012) 1367–1373, https://doi.org/10.1016/j.proeng.2012.07.323.
[91] M.R. Delsouz Khaki, M.S. Shafeeyan, A.A.A. Raman, W.M.A.W. Daud, Evaluating the efficiency of nano-sized Cu doped TiO2/ZnO photocatalyst under visible light irradiation, J. Mol. Liq. 258 (2018) 354–365, https://doi.org/10.1016/j.molliq.2017.11.030.